

Title: Abundance compensates kinetics: Similar effect of dopamine signals on D1 and D2 receptor populations

Abbreviated title: Dopamine receptor abundance compensates kinetics

Lars Hunger¹, Arvind Kumar², Robert Schmidt¹

¹Department of Psychology, University of Sheffield, UK

²Computational Science and Technology, School of Electrical Engineering and Computer Science, KTH Royal Institute of Technology, Stockholm, Sweden

Corresponding author:

Lars Hunger

Department of Psychology, University of Sheffield, UK

pc4xlh@sheffield.ac.uk, Lars.Hunger.314@gmail.com

Number of pages: 40

Number of figures: 11

Number of tables: 1

Number of words for Abstract: 194

Number of words for Introduction: 688

Number of words for Discussion: 1020

Conflict of Interest: The authors declare no competing financial interests.

Acknowledgements: We thank Joshua Berke, Paul Overton, Alejandro Jimenez, Mohammadreza Mohagheghi Nejad and Amin Mirzaei for helpful discussions. This work was supported by the University of Sheffield and its high performance computing resources, by funding from the EU H2020 Programme as part of the Human Brain Project (HBP-SGA1, 720270; HBP-SGA2, 785907), and the BrainLinks-BrainTools Cluster of Excellence funded by the German Research Foundation (DFG, grant number EXC 1086), and the state of Baden-Wuerttemberg through bwHPC.

Abstract

The neuromodulator dopamine plays a key role in motivation, reward-related learning and normal motor function. The different affinity of striatal D1 and D2 dopamine receptor types has been argued to constrain the D1 and D2 signalling pathways to phasic and tonic dopamine signals, respectively. However, this view assumes that dopamine receptor kinetics are instantaneous so that the time courses of changes in dopamine concentration and changes in receptor occupation are basically identical. Here we developed a neurochemical model of dopamine receptor binding taking into account the different kinetics and abundance of D1 and D2 receptors in the striatum. Testing a large range of behaviorally-relevant dopamine signals, we found that the D1 and D2 dopamine receptor populations responded very similarly to tonic and phasic dopamine signals. Furthermore, due to slow unbinding rates, both receptor populations integrated dopamine signals over a timescale of minutes. Our model provides a description of how physiological dopamine signals translate into changes in dopamine receptor occupation in the striatum, and explains why dopamine ramps are an effective signal to occupy dopamine receptors. Overall, our model points to the importance of taking into account receptor kinetics for functional considerations of dopamine signalling.

Significance statement

1 Current models of basal ganglia function are often based on a distinction of two types of
2 dopamine receptors, D1 and D2, with low and high affinity, respectively. Thereby, phasic
3 dopamine signals are believed to mostly affect striatal neurons with D1 receptors, and tonic
4 dopamine signals are believed to mostly affect striatal neurons with D2 receptors. This view
5 does not take into account the rates for the binding and unbinding of dopamine to D1 and
6 D2 receptors. By incorporating these kinetics into a computational model we show that D1
7 and D2 receptors both respond to phasic and tonic dopamine signals. This has implications
8 for the processing of reward-related and motivational signals in the basal ganglia.

9 Introduction

10 The neuromodulator dopamine (DA) plays a key role in motivation, reward-related learning
11 and normal motor function. Many aspects of DA function are mediated by its complex effects
12 on the excitability (Day et al., 2008) and strength of cortico-striatal inputs (Reynolds et al.,
13 2001) in the context of motor control (Syed et al., 2016), action-selection (Redgrave et al.,
14 2010), reinforcement learning (Schultz, 2007), and addiction (Everitt and Robbins, 2005).
15 The striatal DA concentration ([DA]) can change over multiple timescales (Schultz, 2007).
16 Fast, abrupt increases in [DA] lasting for $\approx 1 - 3s$ result from phasic bursts in DA neurons
17 (Roitman et al., 2004), which signal reward-related information (Schultz, 2007; Grace et al.,
18 2007). Slightly slower [DA] ramps occur as animals approach a goal location (Howe et al.,
19 2013) or perform a reinforcement learning task (Hamid et al., 2016). Finally, slow tonic
20 spontaneous firing of DA neurons may control the baseline [DA] and change on a timescale
21 of minutes or longer (Grace et al., 2007). However, whether e.g. learning and motivation
22 are mediated by different timescales of DA cell firing (Niv et al., 2007) has recently been
23 challenged (Berke, 2018; Mohebi et al., 2019). The issue of DA signalling time scales is
24 important because the two main types of DA receptors, D1 and D2, may react to different
25 timescales of the DA signal because of their different affinities for DA.

26 Based on the different DA affinities of D1 and D2 receptors (D1R and D2R), it is often
27 assumed that striatal medium spiny neurons (MSNs) respond differently to tonic and phasic
28 DA signals, depending on which DA receptor type they predominantly express (Dreyer et al.,
29 2010; Surmeier et al., 2007; Grace et al., 2007; Schultz, 2007; Frank and O'Reilly, 2006).
30 According to this "affinity-based" model, the low affinity D1Rs (i.e. with a high dissociation
31 constant $K_D^{D1} = 1.6\mu M$; Richfield et al., 1989) cannot detect tonic changes in [DA] because
32 the fraction of occupied D1Rs is too small ($\approx 1\%$) at a baseline [DA] of $20nM$ and does not
33 change much during tonic, low amplitude [DA] changes. However, D1Rs can detect phasic,
34 high amplitude [DA] increases because they only saturate at a very high [DA]. By contrast,
35 D2Rs have a high affinity (i.e. a low dissociation constant $K_D^{D1} = 25nM$; Richfield et al.,
36 1989) leading to $\approx 40\%$ of D2Rs being occupied at a baseline [DA] of $20nM$. Due to their high
37 affinity, D2Rs can detect low amplitude, tonic increases/decreases in [DA]. However, as D2Rs
38 saturate at relatively low $[DA] > 2 \cdot K_D^{D2}$, and are therefore unable to detect high amplitude,
39 phasic increases in [DA]. This suggests that D1 and D2 type MSNs respond differently to

40 phasic and tonic changes in [DA], solely because of the different affinities of D1Rs and D2Rs
41 (Schultz, 2007). However, this model neglects other factors relevant for receptor occupation
42 and is also incompatible with recent findings that D2R expressing MSNs can detect phasic
43 changes in [DA] (Marcott et al., 2014; Yapo et al., 2017).

44 The affinity-based model assumes that the reaction equilibrium is reached instantaneously,
45 whereby the receptor binding affinity can be used to approximate the fraction of receptors
46 bound to DA. However, this assumption holds only if the receptor kinetics are fast compared
47 to the timescale of the DA signal, which is typically not the case. For instance, D1Rs and
48 D2Rs unbind from DA with a half-life time of $t_{1/2} \approx 80s$ (Burt et al., 1976; Sano et al.,
49 1979; Maeno, 1982; Nishikori et al., 1980), much longer than phasic signals of a few seconds
50 (Robinson et al., 2001; Schultz, 2007; Hamid et al., 2016). Moreover, the fraction of bound
51 receptors might be a misleading measure for the effect of DA signals, since the abundances of
52 D1R and D2R in the striatum are quite different. To investigate the role of receptor kinetics
53 and abundances for DA signalling in the striatum, we developed a neurochemical model of
54 incorporating kinetics and abundances of D1Rs and D2Rs and re-evaluated current views on
55 DA signalling in the striatum. We show that when receptor kinetic timescales are slower
56 than, or comparable to, the DA signalling timescales, the response of D1 and D2 DA receptor
57 populations is similar to each other for both phasic and tonic inputs.

58 Methods and Materials

59 Code Accessibility

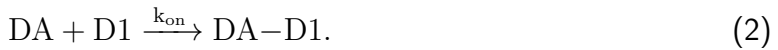
60 All models were implemented in Python. The models and all scripts used to generate the data
61 and figures can be accessed here:
62 https://bitbucket.org/Narur/abundance_kinetics/src/ .

63 Kinetics model

64 In the affinity-based model the receptor kinetics are instantaneous, so that the fraction of
65 occupied D1 and D2 receptors (f_{D1} and f_{D2}) are calculated directly from the concentration
66 of free DA in the extracellular space, $[DA]$, and the dissociation constant K_D (see e.g.
67 Copeland 2004):

$$f = \frac{[DA]}{K_D + [DA]}. \quad (1)$$

68 However, the dissociation constant is an equilibrium constant, so it should only be used for
69 calculating the receptor occupancy when the duration of the DA signal is longer than the
70 time needed to reach the equilibrium. As this is typically not the case for phasic DA signals,
71 since the half-life time of receptors is longer (Burt et al., 1976; Sano et al., 1979; Maeno,
72 1982; Nishikori et al., 1980) than the timeframe of phasic signaling (Roitman et al., 2004),
73 we developed a model which incorporates slow kinetics. When DA and one of its receptors
74 are both present in a solution they constantly bind and unbind. During the binding process a
75 receptor ligand complex (here called DA–D1 or DA–D2) is formed (see e.g. Copeland 2004).
76 We refer to the receptor ligand complex as an occupied DA receptor. Below we provide
77 the model equations for D1 receptors, but the same equations apply for D2 receptors (with
78 different kinetic parameters). In a solution binding occurs when receptor and ligand meet due
79 to diffusion, with high enough energy and a suitable orientation, described as:



80 Accordingly, unbinding of the complex is denoted as:



81 The kinetics of this binding and unbinding, treated here as first-order reactions, are governed
82 by the rate constants k_{on} and k_{off} that are specific for a receptor ligand pair and temperature
83 dependent. Since both processes are happening simultaneously we can write this as:



84 The rate at which the receptor is occupied depends on $[DA]$, the concentration of free receptor
85 $[D1]$ and the binding rate constant k_{on} :

$$\frac{d[DA - D1]}{dt}^+ = k_{on} \cdot [DA] \cdot [D1]. \quad (5)$$

86 The rate at which the receptor-ligand complex unbinds is given by the concentration of the
87 complex $[DA - D1]$ and the unbinding rate constant k_{off} :

$$\frac{d[DA - D1]}{dt}^- = -k_{off} \cdot [DA - D1]. \quad (6)$$

88 The equilibrium is reached when the binding and unbinding rates are equal, so by combining
89 Eq. 5 and Eq. 6 we obtain:

$$k_{on} \cdot [DA] \cdot [D1] = k_{off} \cdot [DA - D1]. \quad (7)$$

90 At the equilibrium the dissociation constant K_D is defined as:

$$K_D = \frac{[DA] \cdot [D1]}{[DA - D1]} = \frac{k_{off}}{k_{on}}. \quad (8)$$

91 When half of the receptors are occupied, i.e. $[DA - D1] = [D1]$, Eq. 8 simplifies to $K_D =$
92 $[DA]$. So at equilibrium, K_D is the ligand concentration at which half of the receptors are
93 occupied.

94 Importantly, for fast changes in $[DA]$ (i.e. over seconds) it takes some time until the changed
95 binding (Eq. 5) and unbinding rates (Eq. 6) are balanced, so the new equilibrium will not be
96 reached instantly. The timescale in which equilibrium is reached can be estimated from the
97 half-life time of the bound receptor. The half-life time assumes an exponential decay process
98 as described in Eq. 6 and is the time required so that half of the currently bound receptors
99 unbind. If $[DA] = 0$, and there is no more binding, the half life time of the receptors can
100 be calculated from the off-rate by using $t_{1/2} = \ln(2)/k_{off}$. Signal durations should be of
101 the same order of magnitude (or longer) than the half-life time in order for the affinity-based
102 model with instant kinetics to be applicable.

103 We calculated the time course of occupied receptor after an abrupt change in $[DA]$ by inte-
104 grating the rate equation, given by the sum of Eq. 5 and Eq. 6:

$$\frac{d[DA - D1]}{dt} = k_{on}[DA][D1] - k_{off}[DA - D1]. \quad (9)$$

105 To integrate Eq. 9 we substitute

$$[D1] = [D1^{tot}] - [DA - D1] \quad (10)$$

106 where $[D1^{tot}]$ is the total amount of D1 receptor (bound and unbound to DA) on the cell
107 membranes available for binding to extracellular DA.

108 To model the effect of phasic changes in [DA] we choose the initial receptor occupancy
 109 $[DA - D1](t = 0) = [DA - D1]^0$ and the receptor occupancy for the new equilibrium at time
 110 infinity $[DA - D1](t = \infty) = [DA - D1]^{\infty}$ as the boundary conditions. With these boundary
 111 conditions we get an analytic expression for the time evolution of the receptor occupancy under
 112 the assumption that binding to the receptor does not significantly change the free [DA]:

$$[DA - D1](t) = ([DA - D1]^0 - [DA - D1]^{\infty}) \cdot e^{-(k_{on}[DA] + k_{off})t} + [DA - D1]^{\infty}. \quad (11)$$

113 For arbitrary DA time courses we solve Eq. 9 for each receptor type numerically employing a
 114 4th order Runge Kutta solver with a 1 ms time resolution.

115 We did not take into account the change in [DA] caused by the binding and unbinding to the
 116 receptors since the rates at which DA is removed from the system by binding to the receptors
 117 is much slower than the rate of DA being removed from the system by uptake through DA
 118 transporters. For example, the rate at which DA binds to the receptors is:

$$\frac{[DA - D1] + [DA - D2]}{dt} = k_{on}^{D1}[DA][D1] + k_{on}^{D2}[DA][D2] = -\frac{[DA]}{dt}. \quad (12)$$

119 For $[DA] = 1\mu M$ with a D1 and D2 occupancy of $[DA - D1] \approx 20.0nM$ and $[DA - D2] \approx$
 120 $40nM$ (the equilibrium values for the baseline $[DA] = 20nM$) and $k_{on}^{D1} = 5.2 \cdot 10^{-6}nM^{-1}s^{-1}$,
 121 $k_{on}^{D2} = 3.3 \cdot 10^{-4}nM^{-1}s^{-1}$, $[D1] \approx 1600.0nM$ and $[D2] \approx 40.0nM$ the rate of DA removal
 122 through binding to the receptors is:

$$\frac{[DA]}{dt}^{binding} = -23.6nM/s. \quad (13)$$

123 However, the DA removal rate by Michaelis-Menten uptake through the DA transporters at
 124 this concentration would be:

$$\frac{[DA]}{dt}^{uptake} = V_{max} \frac{[DA]}{[DA] + K_m} \quad (14)$$

$$= -4.0 \frac{\mu M}{s} \cdot \frac{1\mu M}{1\mu M + 0.21\mu M} \quad (15)$$

$$= -3.3 \frac{\mu M}{s}. \quad (16)$$

125 V_{max} is the maximal uptake rate, and K_m the Michaelis-Menten constant describing the $[DA]$
126 concentration at which uptake is at half the maximum rate. As $\left| \frac{[DA]}{dt}^{uptake} \right| \gg \left| \frac{[DA]}{dt}^{binding} \right|$,
127 the DA dynamics are dominated by the uptake process and not by binding to the recep-
128 tors. Therefore, we neglected the receptor-ligand binding for the DA dynamics in our model.
129 However, for faster DA receptors this effect would become more important.

130 Receptor parameters

131 An important model parameter is the total concentration of the D1 and D2 receptors on
132 the membrane ($[D1]^{tot}$ and $[D2]^{tot}$) that can bind to DA in the extracellular space of the
133 striatum. Our estimate of $[D1]^{tot}$ and $[D2]^{tot}$ is based on radioligand binding studies in the
134 rostral striatum (Richfield et al., 1989, 1987). We use the following equation, in which X is
135 a placeholder for the respective receptor type, to calculate these concentrations.

$$[DX]^{tot} = [DX]^m \cdot \frac{\epsilon \cdot f_{DX}^m}{\alpha \rho_b} \quad (17)$$

136 The experimental measurements provide us with the number of receptors per unit of protein
137 weight $[D1]^m$ and $[D2]^m$. To transform these measurements into molar concentrations for our
138 simulations, we multiply by the protein content of the wet weight of the rat caudate nucleus
139 ϵ , which is around 12% (Banay-Schwartz et al., 1992). This leaves us with the amount of
140 protein per g of wet weight of the rat brain. Next we divide by the average density of a rat
141 brain which is $\rho_b = 1.05 \text{ g/ml}$ (DiResta et al., 1990) to find the amount of receptors per
142 unit of volume of the rat striatum. Finally, we divide by the volume fraction α , the fraction
143 of the brain volume that is taken up by the extracellular space in the rat brain, to obtain
144 the receptor concentration of the receptor in the extracellular medium. The procedure ends
145 here for the D1 receptors since there is no evidence that D1 receptors are internalized in the
146 baseline state (Prou et al., 2001). However, a large fraction of the D2 receptors is retained
147 in the endoplasmatic reticulum of the neuron (Prou et al., 2001), reducing the amount of
148 receptors that contribute to the concentration of receptors in the extracellular medium by f^m ,
149 the fraction of receptors protruding into the extracellular medium.

150 In addition to the receptor concentration, the kinetic constants of the receptors are key
151 parameters in our slow kinetics model. In an equilibrium measurement in the canine cau-

date nucleus the dissociation constant of low affinity DA binding sites, corresponding to D1 receptors (Maeno, 1982), has been measured as $K_D = 1.6\mu M$ (Sano et al., 1979). However, when calculating K_D (using Eq. 8) from the measured kinetic constants (Sano et al., 1979) the value is $K_D^{D1} = 2.6\mu M$. To be more easily comparable to other simulation works (Dreyer et al., 2010) and direct measurements (Richfield et al., 1989; Sano et al., 1979) we choose $K_D^{D1} = 1.6\mu M$ in our simulations. For this purpose we modified both the $k_{on}^{D1} = 0.00025min^{-1}nM^{-1}$ and $k_{off}^{D1} = 0.64min^{-1}$ rate measured (Sano et al., 1979) by $\approx 25\%$, making $k_{on}^{D1} = 0.0003125min^{-1}nM^{-1}$ slightly faster and $k_{off}^{D1} = 0.5min^{-1}$ slightly slower, so that the resulting $K_D^{D1} = 1.6\mu M$. The kinetic constants have been measured at $30^\circ C$ and are temperature dependent. In biological reactions a temperature change of $10^\circ C$ is usually associated with a change in reaction rate around a factor of 2-3 (Reyes et al., 2008). However, the conclusions of this paper do not change for an increase in reaction rates by a factor of 2 – 3 (see **Fig. 9**). It should also be noted that the measurements of the commonly referenced K_D (Richfield et al., 1989) have been performed at room temperature.

The kinetic constants for the D2 receptors were obtained from measurements at $37^\circ C$ of high affinity DA binding sites (Burt et al., 1976), which correspond to the D2 receptor (Maeno, 1982). The values are $k_{on}^{D2} = 0.02min^{-1}nM^{-1}$ and $k_{off}^{D2} = 0.5min^{-1}$, which yields $K_D^{D2} = 25nM$, in line with the values measured in (Richfield et al., 1989). As the off-rate of the D1 and D2 receptors $k_{off}^{D1} = 0.64min^{-1}nM^{-1}$ and $k_{off}^{D2} = 0.5min^{-1}$ is quite similar, the difference in $K_D^{D2} = 25nM$ and $K_D^{D1} = 1.6\mu M$ is largely due to differences in the on-rate of the receptors. This is important because the absolute rate of receptor occupancy depends linearly not only on the on-rate, but also on the receptor concentration (see Eq. 5), which means that a slower on-rate could be compensated for by a higher number of receptors.

The parameters used in the simulations are summarized in Tab. 1.

176 **Dopamine signals**

In our model we assumed a baseline [DA] of $[DA]^{tonic} = 20 nM$ (Dreyer et al., 2010; Dreyer, 2014; Venton et al., 2003; Suaud-Chagny et al., 1992; Borland et al., 2005; Justice Jr, 1993; Atcherley et al., 2015). We modelled changes in [DA] to mimic DA signals observed in experimental studies. We use three types of single pulse DA signals: (long-)bursts, burst-

181 pauses, and ramps.

182 The (long-)burst signal mimics the effect of a phasic burst in the activity of DA neurons in
183 the SNc, e.g. in response to reward-predicting cues (Pan et al., 2005). The model burst signal
184 consists of a rapid linear $[DA]$ increase (with an amplitude $\Delta[DA]$ and rise time t_{rise}) and a
185 subsequent return to baseline. The return to baseline is governed by Michaelis Menten kinetics
186 with appropriate parameters for the dorsal striatum $V_{max} = 4.0 \mu M s^{-1}$ and $K_m = 0.21 \mu M$
187 (Bergstrom and Garris, 2003) and the nucleus accumbens $V_{max} = 1.5 \mu M s^{-1}$ (Dreyer and
188 Hounsgaard, 2013). In our model the removal of DA is assumed to happen without further
189 DA influx into the system (baseline firing resumes when $[DA]$ has returned to its baseline
190 value). Unless stated otherwise, the long-burst signals are used with a $\Delta[DA] = 200 nM$
191 and a rise time of $t_{rise} = 0.2 s$ at $V_{max} = 1.5 \mu M s^{-1}$, similar to biologically realistic transient
192 signals (Cheer et al., 2007; Robinson et al., 2001; Day et al., 2007).

193 The burst-pause signal has two components, an initial short, small amplitude burst ($\Delta[DA] =$
194 $100 nM$, $t_{rise} = 0.1 s$), with the corresponding $[DA]$ returning then to baseline (as for the
195 long burst above). However, there is a second component in the DA signal, in which $[DA]$
196 falls below baseline, simulating the effect of a pause in DA neuron firing. The length of this
197 firing pause is characterized by the parameter t_{pause} . This burst-pause $[DA]$ signal reflects the
198 DA cell firing pattern consisting of a brief burst followed by a pause in activity (Pan et al.,
199 2008; Schultz, 2016).

200 The ramp DA signal is characterized by the same parameters as the burst pattern, but with
201 a longer t_{rise} , and a smaller $\Delta[DA]$ (parameter settings provided in each simulation).

202 For the simulations comparing the area under the curve of the input DA signal with the
203 resulting receptor occupancy (**Fig. 5**) we used the burst, burst-pause, and ramp signals de-
204 scribed above with a range of parameter settings. For the burst DA signal we used amplitudes
205 $\Delta[DA]^{max}$ of 50, 100, 150, 200, 250, 300, 350, 400, 500, 600, 700, 800, 900, and 1000 nM.
206 For the ramping DA signals we used rise times t_{rise} of 0.2, 0.5, 1.0, 1.5, 2.0, 3.0, 4.0, 5.0,
207 6.0, and 7.0 s, For the burst-pause DA signal we different values for V_{max} of 1.0, 1.5, 2.0,
208 2.5, 3.0, 2.5, and $4.0 \mu M s^{-1}$.

209 Behavioural task simulation

210 To determine whether DA receptor occupancy can integrate reward signals over minutes,
211 we simulated experiments consisting of a sequence of 50 trials. In each sequence the reward
212 probability was fixed. The trials contained either a (long-)burst DA signal (mimicking a reward)
213 or a burst-pause DA signal (mimicking no reward) at the beginning of the trial according to
214 the reward probability of the sequence. The inter-trial interval was $15 \pm 5\text{s}$ (**Fig. 8**). We
215 choose this highly simplistic scenario to mimic DA signals in a behavioural task in which the
216 animal is rewarded for correct performance. However, here the specifics of the task are not
217 relevant as our model addresses the integration of the DA receptor occupancy over time.
218 Although we chose to use the burst-pause type signal as shown in **Fig. 2a** as a non-rewarding
219 event, the difference to a non-signal are minimal after the end of the pause (**Figs. 3 and**
220 **4**). Each sequence started from a baseline receptor occupancy, assuming a break between
221 sequences long enough for the receptors to return to baseline occupancy (around 5 minutes).
222 For the simulations shown in **Fig. 4** all trials started exactly 15 s apart.
223 While for the simulations shown in **Fig. 4** the sequence of DA signals was fixed, we also
224 simulated a behavioural task with stochastic rewards (**Fig. 8**). There we simulated reward
225 probabilities from 0% to 100% in 10% steps. For each reward probability we ran 500 se-
226 quences, and calculated the mean receptor occupancy over time (single realizations shown in
227 **Fig. 8a, c**). To investigate whether the receptor occupancy distinguished between different
228 reward probabilities we applied a simple classifier to the receptor occupancy time course.
229 The classifier was used to compare two different reward probabilities at a time. At each time
230 point during the simulated experiment it was applied to a pair of receptor occupancies, e.g. one
231 belonging to a 50% and one to a 30% reward probability sequence. For each sequence the
232 classifier assigned the current receptor occupancy to the higher or lower reward probability
233 depending on which reward probabilities mean (over 500 sequences) receptor occupancy was
234 closer to the current receptor occupancy. As we knew the underlying reward probability of
235 each sequence we were able to calculate the true and false positive rates and accuracy for
236 each time point in our set of 500 sequences for both the D1R and D2R (**Fig. 8e, f**). The
237 accuracy was calculated based on all time points between 200 and 800s within a sequence to
238 avoid the effect of the initial “swing-in” and post-sequence DA levels returning to baseline.

239 Results

240 Before investigating the role of the receptor kinetics in response to different DA signals, we
241 started by establishing the receptor binding at baseline [DA], taking into account the different
242 numbers of D1 and D2 receptors in the striatum. For a stable baseline [DA] the receptor
243 affinities can be used to calculate receptor occupation (see Methods, Eq. 1).

244 First, we investigated receptor binding for a range of affinities (**Fig. 1**), reflecting the range
245 of measured values in different experimental studies (Neve and Neve, 1997). We report the
246 resulting receptor occupancy in terms of the concentration of D1Rs and D2Rs bound to DA
247 (denoted as $[D1 - DA]$ and $[D2 - DA]$, respectively). Due to the low affinity of D1Rs, at
248 low baseline [DA] only a small fraction of D1 receptors may be occupied. However, there are
249 overall more D1Rs than D2Rs (Richfield et al., 1989), and $\approx 80\%$ of D2Rs are retained in
250 the endoplasmatic reticulum (Prou et al., 2001). Therefore, the concentration of D1Rs in
251 the membrane available to extracellular DA is a lot higher than the concentration of D2Rs
252 (e.g. 20 times more in the nucleus accumbens; Nishikori et al., 1980; see Methods). Thus,
253 in our simulation, the actual concentration of bound D1Rs ($[D1 - DA] \approx 20nM$) was, at
254 DA baseline, much closer to the concentration of bound D2Rs ($[D2 - DA] \approx 35nM$) than
255 suggested by the different D1 and D2 affinities alone. We further confirmed that this was
256 not due to a specific choice of the dissociation constants in the model, as $[D1 - DA]$ and
257 $[D2 - DA]$ remained similar over the range of experimentally measured D1R and D2R affinities
258 (Neve and Neve, 1997) (**Fig. 1a**). This suggests that $[D1 - DA]$ is at most twice as high
259 as $[D2 - DA]$ instead of 40 times higher as suggested by the difference in fraction of bound
260 receptors. Therefore, $[D1 - DA]$ and $[D2 - DA]$ might be better indicators for the signal
261 transmitted to MSNs, as the fraction of bound receptors neglects the different receptor type
262 abundances.

263 Next, we investigated the effect of slow [DA] changes (Grace, 1995; Schultz, 1998; Floresco
264 et al., 2003) by exposing our model to changes in the [DA] baseline. For signalling timescales
265 that are long with respect to the half-life time of the receptors ($t_{slow} \gg t_{1/2} \approx 80s$), we
266 used the dissociation constant to calculate the steady state receptor occupancy. We found
267 that for a range of [DA] baselines (mimicking slow changes in [DA]), there was less than
268 two-fold difference between $[D1 - DA]$ and $[D2 - DA]$ (**Fig. 1b**), because of the different

269 abundances of D1 and D2 receptors. This is in contrast to affinity-based models, which
270 suggest that D2Rs are better suited to encode slow or tonic changes in [DA]. Interestingly
271 the change of $[D1 - DA]$ was almost linear in [DA], while the change of $[D2 - DA]$ showed
272 nonlinear effects due to the change in available free D2R. Thus, based on these results, it
273 could even be argued that D1Rs are better at detecting tonic signals at high [DA] levels, since
274 they do not saturate as easily.

275 While for baseline and slow changes in [DA] the receptor occupation can be determined based
276 on the receptor affinity, fast changes in [DA] also require a description of the underlying
277 receptor kinetics. To investigate the effect of typical DA signals on receptor occupation,
278 we developed a kinetics model incorporating binding and unbinding rates that determine the
279 overall receptor affinity (see Methods, Eq. 8, 9). The available experimental measurements
280 indicate that the different D1R and D2R affinities are largely due to different binding rates,
281 while their unbinding rates are similar (Burt et al., 1976; Sano et al., 1979; Maeno, 1982;
282 Richfield et al., 1989). We incorporated these measurements into our kinetics model and
283 investigated the model's response to a variety of fast DA signals.

284 We started by measuring the model response to a [DA] step change from 20nM to $1\mu\text{M}$.
285 This is quite a large change compared to phasic DA signals *in vivo* (Robinson et al., 2001;
286 Cheer et al., 2007; Hamid et al., 2016), which we choose to illustrate that our results are not
287 just due to a small amplitude DA signal. We found that binding to both receptor subtypes
288 increased very slowly. Even for the high affinity D2Rs it took more than 5s to reach their new
289 equilibrium (**Fig. 1c**). Thus, unlike the affinity-based model, our model suggests that the
290 D2Rs will not saturate for single reward events, which last overall for up to $\approx 3\text{s}$. Note that
291 the non-saturation is independent of the abundance of the receptors and is only determined
292 by the kinetics of the receptors (see Methods). Due to their slow unbinding, D1Rs and
293 D2Rs also took a long time to return to baseline receptor occupancy after a step down from
294 $[DA] = 1\mu\text{M}$ to $[DA] = 20\text{nM}$ (**Fig. 1d**). Thus, we conclude that with slow kinetics of
295 receptor binding both D1Rs and D2Rs can detect single phasic DA signals and that both
296 remain occupied long after a high [DA] has returned to baseline.

297 DA receptor binding kinetics for different types of DA signals

298 Next, we investigated $[D1 - DA]$ and $[D2 - DA]$ for three different types of DA signals
299 (**Fig. 2**). The first signal was a phasic DA increase ('long burst', **Fig. 2a**), mimicking responses
300 to rewards and reward-predicting stimuli (Robinson et al., 2001; Cheer et al., 2007). The
301 second signal was a brief phasic DA increase, followed by a decrease ('burst-pause', **Fig. 2a**),
302 mimicking responses to conditioned stimuli during extinction (Pan et al., 2008) or to other
303 salient stimuli (Schultz, 2016). The third signal was a prolonged DA ramp, mimicking a value
304 signal when approaching a goal (Howe et al., 2013; Hamid et al., 2016) (**Fig. 2b**). In the
305 affinity-based model with instant kinetics the D1Rs mirrored the [DA] time course for all three
306 types of signals, since even at $[DA] = 200nM$ D1Rs are far from saturation. By contrast,
307 D2Rs showed saturation effects as soon as $[DA] > 2 \cdot K_D^{D2}$, leading to differing D1 and D2
308 time courses (**Fig. 2**, middle and bottom rows, grey traces). Importantly, in our model with
309 slow kinetics, the time courses of $[D1 - DA]$ and $[D2 - DA]$ were nearly identical, supporting
310 that both receptor types are equally affected by phasic DA signals. This was the case for all
311 the three signals: burst, burst-pause and ramping DA signals. The only difference between
312 the $[D1 - DA]$ and $[D2 - DA]$ time courses were the absolute amplitudes. For example,
313 $[D2 - DA]$ started from a baseline about twice as high as $[D1 - DA]$, but then also responded
314 to the long burst DA signal with a change about twice as high. The similarity of $[D1 - DA]$
315 and $[D2 - DA]$ responses to both slow (**Fig. 1b**) and fast (**Fig. 2**) [DA] changes indicates
316 that the different DA receptor types respond similarly independent of the timescale of [DA]
317 changes. It could even be argued that D2Rs are better at detecting phasic DA signals, since
318 they respond with a larger absolute change in occupied receptors.

319 To understand why the D1Rs and D2Rs respond in a similar fashion, we considered the
320 relevant model parameters in more detail. The binding rate constants of D1Rs and D2Rs
321 differ by a factor of ≈ 60 ($k_{on}^{D1} = 0.0003125nm^{-1}min^{-1}$ and $k_{on}^{D2} = 0.02nm^{-1}min^{-1}$; Burt
322 et al., 1976; Sano et al., 1979; Maeno, 1982; see also Methods), suggesting faster D2Rs.
323 However, experimental data suggests that there are ≈ 40 fold more unoccupied D1 receptors
324 ($[D1] \approx 1600nM$) than unoccupied D2 receptors ($[D2] \approx 40nM$) on MSN membranes in
325 the extracellular space of the rat striatum (Nishikori et al., 1980). Therefore, the absolute
326 binding rate $\frac{d[DX-DA]}{dt}^+ = k_{on} \cdot [DA] \cdot [DX]$ differs only by a factor of ≈ 1.5 between the D1Rs
327 and D2Rs. That is, the difference in the kinetics of D1Rs and D2Rs is compensated by the

328 different receptor numbers, resulting in nearly indistinguishable aggregate kinetics (**Fig. 2**).
329 This is consistent with recent experimental findings which showed that D2R expressing MSNs
330 can detect phasic [DA] signals (Marcott et al., 2014; Yapo et al., 2017).

331 The dynamics introduced by the slow kinetics in our model also affected the time course of DA
332 signalling. With instant kinetics the maximum receptor occupancy was reached at the peak
333 [DA] (**Fig. 2**, middle and bottom rows). By contrast, for slow kinetics the maximum receptor
334 occupancy was reached when [DA] returned to its baseline (**Fig. 2a**) because as long as [DA]
335 was higher than the equilibrium value of [D1-DA] and [D2-DA], more receptors continued
336 to become occupied. Therefore, for all DA signals, the maximum receptor occupancy was
337 reached towards the end of the pulse.

338 Another striking effect of incorporating receptor kinetics was that a phasic increase in [DA]
339 kept the receptors occupied for a long time (**Fig. 2a** green traces). However, when a phasic
340 increase was followed by a decrease, [D1-DA] and [D2-DA] returned to baseline much faster
341 (**Fig. 2a** purple traces). This indicates that burst-pause firing patterns can be distinguished
342 from pure burst firing patterns on the level of the MSN DA receptor occupancy. This supports
343 the view that the fast component of the DA firing patterns (Schultz, 2016) is a salience
344 response, and points to the intriguing possibility that the pause following the burst can, at
345 least partly, revoke the receptor-ligand binding induced by the burst. In fact, for each given
346 burst amplitude, a sufficiently long pause duration can cancel the receptor activation (**Fig. 3**),
347 with larger [DA] amplitudes requiring longer pauses to cancel the activation. Thereby, the
348 burst-pause firing pattern of DA neurons could effectively signal a reward “false-alarm”.

349 The long time it took [D1-DA] and [D2-DA] to return to baseline after phasic DA signals
350 (**Fig. 2a**) indicates that the receptor occupation integrates DA signals over time. To examine
351 this property, we simulated a sequence of DA signals on a timescale relevant for behavioural
352 experiments (**Fig. 4**). Each sequence consisted of 50 events and each event was separated
353 by 15 s. Three different types of sequences were tested: 50 phasic DA bursts, 40 phasic DA
354 bursts followed by 10 burst-pause signals, and 40 phasic DA bursts followed by 10 non-events.
355 We found that both [D1-DA] and [D2-DA] accumulated over the sequence of DA signals.
356 The sawtooth shape of the curves was due to the initial unbinding of the receptors, which
357 was then interrupted by the next DA signal 15 s later. At higher levels of receptor activation,
358 the amount of additional activated receptor per DA pulse was reduced since there are less

359 free receptors available, and the amount of receptors unbinding during the pulse duration was
360 increased because more receptors were occupied. The accumulation occurred as long as the
361 time interval between the DA signals was shorter than $\approx 2 \cdot t_{1/2}$. Together, the shape and
362 period of the DA pulses lead to the formation of an equilibrium, visible here as a plateau for
363 the absolute amount of occupied receptor. This occurred at the level at which the amount of
364 receptors unbinding until the next DA burst was the same as the amount of receptors getting
365 occupied by the DA burst. Finally, the burst-pause events did not lead to an accumulation of
366 occupied receptors over time. In fact, the receptor occupation was the same for burst-pause
367 and non-event, except during the short burst component of the burst-pause events (note the
368 overlapping green and orange curves in **Fig. 4**). This extends the property of burst-pause
369 signals as “false alarm” signals to a wide range of occupancy levels.

370

371 Incorporating the slow kinetics in the model is crucial for functional considerations of the DA
372 system. Currently, following the affinity-based model, the amplitude of a DA signal (i.e. peak
373 [DA]) is often considered as a key signal, e.g. in the context of reward magnitude or probability
374 (Morris et al., 2004; Tobler et al., 2005; Hamid et al., 2016). However, as DA unbinds slowly
375 (over tens of seconds; **Fig. 1d**) and the binding rate changes approximately linearly with
376 [DA], the amount of receptor occupancy does not primarily depend on the amplitude of
377 the [DA] signal. Due to the linearity of the binding rate, the receptor occupation increases
378 linearly with time and $[DA] - [DA]_{\text{baseline}}$, while the unbinding is negligible as long as $t \ll t_{1/2}$.
379 Therefore the integral of the [DA] time course should be a close approximation of the receptor
380 occupation for signals that are shorter than the half-life time of the receptors. We confirmed
381 this consideration by simulating a range of DA signals (burst, burst-pauses, and ramps) with
382 different durations and amplitudes. For each DA signal we compared its area under the curve
383 with the resulting peak change in the absolute receptor occupancy. For both D1R and D2R
384 we found that the maximum receptor activation was proportional to the area under the curve
385 of the [DA] signal, while independent of its specific time course (**Fig. 5**). The small deviation
386 from the proportionality seen for large-area DA signals for the D2Rs (**Fig. 5b**) was due to
387 the decrease in the amount of free receptor as more and more receptors were bound. In this
388 regime the assumption that the binding rate is linear with [DA] was slightly violated leading

389 to the non-proportionality. The overall striking proportionality of the integral of the DA signal
390 with receptor binding indicates that D1Rs and D2Rs act as slow integrators of the DA signal.
391 Interestingly, this means that DA ramps, even with a relatively small amplitude (**Fig. 2b** and
392 **Fig. 7**), are an effective signal to occupy DA receptors. In contrast, for locally very high [DA]
393 (e.g. at corticostriatal synapses during phasic DA cell activity; Grace et al., 2007) our model
394 predicts that the high concentration gradient would only lead to a very short duration of this
395 local DA peak and thereby make it less effective in occupying DA receptors.

396 To further test the generality of our findings, we examined our model responses systematically
397 for a set of different DA time courses (**Fig. 6** and **Fig. 7**). While the shape of the DA pulses
398 strongly affected the time courses of the receptor activation, D1 and D2 receptor activation
399 were virtually identical for a given pulse shape. For DA bursts with different amplitudes
400 (**Fig. 6a**), higher amplitudes of the DA burst lead to stronger receptor activation. However,
401 the relationship between burst amplitude and receptor occupation was not linear, but instead
402 reflected the area under the curve of the DA pulse (see above). Importantly, despite 'slow'
403 kinetics, the onset of the increase in $[D1 - DA]$ and $[D2 - DA]$ was immediate and reached
404 relevant levels in a nanomolar range within a few 100 ms. For a fixed burst amplitude, we also
405 determined the effect of different DA re-uptake rates to look at potential differences in DA
406 signalling in dorsal and ventral striatum, with fast and slow re-uptake, respectively. This was
407 done by changing the parameter V_{max} (see Methods), which controlled the time the [DA] took
408 to return to the baseline from the peak value (**Fig. 6b**). While this had only a small visible
409 effect on the input DA signal (**Fig. 6b**, top panel), the resulting $[D1 - DA]$ and $[D2 - DA]$
410 were quite different. This is important because this property is not seen in the affinity-based
411 model, in which the time course of $[D1 - DA]$ and $[D2 - DA]$ would simply follow the input
412 [DA] signal.

413 Next, we examined DA ramps with different time courses, but the same maximal amplitude.
414 Again, consistent with our consideration of the important role of the area under the curve
415 of DA signals, we found that longer ramps lead to larger DA receptor occupation (**Fig. 7a**).
416 We investigated the DA signals that included the effects of pauses in DA cell activity further.
417 First, we tested burst-pause signals and determined the role of the duration of the pause.
418 For a fixed burst amplitude and duration, a different duration of the subsequent pause lead
419 to differing receptor activation levels when the burst-pause signal was over (**Fig. 7b**). This

420 indicates that DA pauses are very effective in driving the receptor occupation quickly back to
421 baseline (i.e. within few seconds) because, in this case, the receptor occupation changes reflect
422 solely the unbinding rates. In contrast, for a burst followed by a return to baseline [DA], the
423 decrease in receptor occupation would be slower because during the baseline portion of the
424 signal both binding and unbinding processes play a role. In this case the binding counteracts
425 some of the unbinding. In this context we also looked at pure DA pauses (i.e. without a
426 preceding burst), e.g. reflecting DA cell responses to aversive stimuli (Schultz, 2007) that
427 lead to reductions in [DA] (Roitman et al., 2008). These signals also lead to fast decreases in
428 [D1-DA] and [D2-DA], with the duration of the pause having a strong effect on the amplitude
429 and duration of the decrease (**Fig. 7c**).

430 D1R and D2R occupancy in a probabilistic reward task paradigm

431 A general effect of the slow kinetics was that DA receptors remained occupied long after the
432 DA pulse was over (**Fig. 2**), so that the effect of DA pulses was integrated over time (**Fig. 4**).
433 To investigate the information that is preserved in the receptor occupation about DA signals on
434 time scales relevant for behavioural tasks, we simulated sequences with probabilistic DA events
435 (see Methods). First, we compared sequences, in which every $15 \pm 5s$ there was a DA burst
436 with either 30%, 50%, or 70% probability (**Fig. 8a, c**). The resulting changes in $[D1 - DA]$
437 and $[D2 - DA]$ confirmed the integration of DA pulses over minutes. The integration of DA
438 bursts was due to DA bursts arriving before the receptor occupation caused by the previous
439 pulses had decayed, leading to an increased receptor activation compared to single DA bursts
440 (**Fig. 4**). We then examined whether the DA receptor occupancy can distinguish different
441 reward probabilities by using a simple classifier comparing two sequences with each other (see
442 Methods). We tested sequences from 0% to 100% probability in steps of 10%, and ordered
443 the resulting classification success in terms of the difference in reward probability between the
444 two sequences (**Fig. 8b, d, e, f**). For example, a comparison between a 30% and a 70%
445 reward probability sequence yields a data point for a 40% difference. For both D1 and D2
446 receptors, we found that already for differences of 10% the classification exceeded chance level,
447 and yielded near perfect classification around a 40% difference. Overall, the classification was
448 slightly better for D1R due to their slower unbinding rate and more stable plateau response
449 (**Fig. 4**). The successful classification of reward probabilities demonstrates that it would be

450 possible for striatal neurons to read out different reward rates from DA receptor occupancy
451 in a behavioural task. This provides a potential neural substrate for how fast DA signals can
452 lead to an encoding of the slower reward rate, which can be utilized as a motivational signal
453 (Mohebi et al., 2019).

454 **Validation for fast binding kinetics**

455 Our model assumption of slow kinetics was based on neurochemical estimates of wildtype DA
456 receptors (Burt et al., 1976; Sano et al., 1979; Maeno, 1982). In contrast, recently developed
457 genetically-modified DA receptors, used to probe [DA] changes, have fast kinetics (Sun et al.,
458 2018; Patriarchi et al., 2018). Although the kinetics of the genetically modified DA receptors
459 are unlikely to reflect the kinetics of the wildtype receptors (see Discussion), we also examined
460 the effect of faster DA kinetics in our model. Fast kinetics were implemented by multiplying
461 k_{on} and k_{off} by a factor q , keeping K_D constant. We found that the similarity between
462 $[D1 - DA]$ and $[D2 - DA]$ persists even if the actual kinetics were a 100 times faster than
463 assumed in our model (Fig. 9). This was the case for all types of [DA] signals because the
464 difference between the aggregate D1 and D2 binding rates (Eq. 5) still only differed by a factor
465 of 1.5. Furthermore, the D2Rs did not show visible saturation effects even for $q = 100$. Faster
466 kinetics mostly affected the amplitude of the receptor response and the time it took to return
467 to baseline receptor occupancy. However, only for $q = 100$ the pauses dropped slightly below
468 baseline receptor occupancy (Fig. 9a, b). On a longer time scale with repetitive DA bursts
469 (Fig. 9e, f) D1Rs and D2Rs integrated the DA bursts over time even if kinetics were twice
470 as fast ($q = 2$). This is because the half-time of the receptors were 40 s (for $q = 2$), while
471 the DA burst signal was repeated every 15 s. Thereby, $[D1-DA]$ and $[D2-DA]$ were dominated
472 by the repetition of the signal rather than by the impact of individual DA burst signals. In
473 contrast, for $q = 10$ the change in receptor occupancy was dominated by the single pulses,
474 since the half-life time was 8s, whereby the receptors mostly unbind in between DA pulses.
475 Therefore, our results concerning the similarity of D1 and D2 receptors do not depend on the
476 exact kinetics parameters or potential temperature effects, as long as the parameter changes
477 are roughly similar for D1 and D2 receptors. However, DA receptor kinetics faster by a factor
478 of 10 or more affected the ability of DA receptor occupancy to integrate DA pulses over time
479 (Fig. 9e, f).

480 In our model we assumed homogeneous receptor populations, namely that all D1 receptors
481 have a low affinity and that all D2 receptors have a high affinity. However, this could be a
482 simplification, as $\approx 10\%$ of D2 receptors may exist in a low affinity state, while $\approx 10\%$ of
483 the D1 receptors may be in a high affinity state (Richfield et al., 1989). Therefore, we also
484 incorporated different affinity states of the D1 and D2 receptors into our model. The D1Rs in
485 a high affinity state ($D1^{high}$) were modelled by increasing the on-rate of the D1R but keeping
486 its off-rate constant, creating a receptor identical to the $D2^{high}$ receptor. Although the high
487 affinity state kinetics of the D1R are currently unknown, we choose this model as a faster on-
488 rate potentially has the strongest effect on our conclusions. Correspondingly, we modelled the
489 $D2^{low}$ receptor as a D2R with slower on-rate, which was equivalent to simply reducing $[D2^{tot}]$
490 since the $D2^{low}$ receptors were predominantly unoccupied during baseline DA and bound only
491 sluggishly to DA during phasic signals. The main effect of incorporating the different receptor
492 affinity states was a change in the respective equilibrium values of absolute concentration of
493 receptors bound to DA (Fig. 10). However, importantly, taking into account these different
494 affinity states, preserved the similarity of time courses of D1R and D2R occupancy and the
495 ability to integrate DA pulses over time (Fig. 10 and Fig. 11) since the half-life time of both
496 receptors remained long.

497 Discussion

498 The functional roles of DA in reward-related learning and motivation have typically been stud-
499 ied by characterizing the firing patterns of dopaminergic neurons and the resulting changes
500 in striatal [DA] (Schultz, 2007). In contrast to other, more conventional neurotransmitters
501 like glutamate or GABA, the release of DA in the striatum may form a global signal that
502 affects large parts of the striatum similarly (Schultz, 1998). Such global [DA] changes involve
503 longer time scales lasting at least several seconds (Roitman et al., 2008; Howe et al., 2013).
504 Importantly, to affect neural activity in the striatum, DA first needs to bind to DA receptors.
505 This process is often simplified by assuming that this happens instantaneously, so that every
506 change in [DA] is immediately translated into a change in DA receptor occupation. As this
507 contradicts physiological measurements of the receptor kinetics (Burt et al., 1976; Sano et
508 al., 1979; Maeno, 1982; Nishikori et al., 1980), we developed and investigated a model incor-

509 porating DA receptor kinetics as well as differences in D1 and D2 receptor abundance in the
510 striatum.

511 Our results cast doubt on several long-held views on DA signalling. A common view is that
512 D1 and D2 MSNs in the striatum respond to different DA signals due to the affinity of their
513 predominant receptor type. Accordingly, phasic DA changes should primarily affect D1 MSNs,
514 while slower changes or DA pauses should primarily affect D2 MSNs. In contrast, our model
515 indicates that both D1R and D2R systems can detect [DA] changes, independent of their
516 timescale, equally well. That is, slow tonic changes in [DA], phasic responses to rewards, and
517 ramping increases in [DA] over several seconds lead to a similar time course in the response
518 of D1 and D2 receptor occupation in our model. However, the baseline level of activated
519 DA receptors and the amplitude of the response was typically twice as high in D2 compared
520 to D1 receptors. Although, D1 and D2 receptors have opposing effects on the excitability
521 (Flores-Barrera et al., 2011) and strength of cortico-striatal synapses (Centonze et al., 2001),
522 we challenge the view that differences in receptor affinity introduce additional asymmetries in
523 D1 and D2 signalling. Instead of listening to different components of the DA signal, D1 and
524 D2 MSNs may respond to the same DA input. This would actually increase the differential
525 effect on firing rate responses of D1 and D2 MSNs because the opposite intracellular effects
526 of D1 and D2 activation (Surmeier et al., 2007) occur then for the whole range of DA signals.

527 Recently, ramps in [DA], increasing over several seconds towards a goal, have been connected
528 to a functional role of DA in motivation (Howe et al., 2013; Hamid et al., 2016). In our
529 model DA ramps were very effective in occupying DA receptors due to their long duration. In
530 contrast, for brief phasic increases, the receptor occupation was less pronounced. Overall, our
531 model predicts that the area under the curve of DA signals determines the receptor activation,
532 which puts more emphasis on the duration of the signals, rather than the amplitude of brief
533 DA pulses.

534 Our model is also relevant for the interpretation of burst-pause firing patterns in DA neurons.
535 These are a different firing pattern than the typical reward-related bursts, and consist of a brief
536 burst followed by a brief pause in action potentials. Such two-component responses of DA
537 cells may reflect saliency and value components, respectively (Schultz, 2016). For example,
538 during extinction learning burst-pause firing patterns have been observed as a response to
539 conditioned stimuli, with each component lasting about 100 ms (Pan et al., 2008). Our

540 model provides a mechanistic account for how the burst–pause DA signals have a different
541 effect on MSNs than pure burst signals, which is important to distinguish potential rewarding
542 signals from other salient, or even aversive stimuli. In our model the pause following the burst
543 was very effective in reducing the number of occupied receptors quickly, thereby preventing
544 the otherwise long-lasting receptor occupation due to the burst. Thereby, canceling the effect
545 of the brief burst might be a neural mechanism to correct a premature burst response that
546 was entirely based on saliency rather than stimulus value (Schultz, 2016). As fast responses
547 of DA cells to potentially rewarding stimuli are advantageous to quickly redirect behaviour,
548 the subsequent pause signal might constitute an effective correction mechanism labelling the
549 burst as a false alarm.

550 Functionally, the slow unbinding rate of D1 and D2 receptors pointed to an interesting property
551 in integrating phasic DA events over time. The unbinding rate might be one of the mechanisms
552 translating fast DA signals into a slower time scale, which could be a key mechanism to
553 generate motivational signals (Mohebi et al., 2019). Importantly, the slow kinetics of receptor
554 binding do not prevent a fast neuronal response to DA signals. In our model [DA] changes
555 affected the number of occupied receptors immediately; it just took seconds or even minutes
556 until the new equilibrium was reached. However, reaching the new equilibrium is not necessarily
557 relevant on a behavioural level. Instead the intracellular mechanisms that react to the receptor
558 activation need to be considered to determine which amount of receptor activation is required
559 to affect neural activity. In our model changes on a nanomolar scale occurred within 100
560 ms, a similar timescale as behavioural effects of optogenetic DA manipulations (Hamid et al.,
561 2016).

562 The slower time scales were introduced into our model by the kinetics based on in-vitro mea-
563 surements (Burt et al., 1976; Sano et al., 1979; Maeno, 1982; Nishikori et al., 1980). A
564 limitation of our model is the uncertainty about the accuracy of these measurements, and
565 whether they reflect in-vivo conditions. We addressed this here by also examining faster ki-
566 netics, for which there is currently no direct evidence in the literature. However, recently DA
567 receptors have been genetically modified to serve as sensors for fast [DA] changes (Patriarchi
568 et al., 2018), which suggests possible fast kinetics. It seems unlikely though that the kinetics
569 of the genetically-modified receptors represent the kinetics of the wildtype DA receptors, as
570 e.g. the screening procedure to find suitable receptor variants yielded a large range of different

571 affinities based on changes at the IL-3 site (Patriarchi et al., 2018). Changes in the IL-3 site
572 have also previously been shown to strongly affect the receptor affinity (Robinson et al., 1994).
573 Our broader view is that it is important to consider the effect of the receptor kinetics on DA
574 signalling, which have not received much attention in experimental studies, nor in theoretical
575 considerations of DA function so far.

576

577 References

578 Atcherley CW, Wood KM, Parent KL, Hashemi P, Heien ML (2015) The coaction of tonic
579 and phasic dopamine dynamics. *Chemical Communications* 51:2235–2238.

580 Banay-Schwartz M, Kenessey A, DeGuzman T, Lajtha A, Palkovits M (1992) Protein content
581 of various regions of rat brain and adult and aging human brain. *Age* 15:51–54.

582 Bergstrom BP, Garris PA (2003) passive stabilizationof striatal extracellular dopamine across
583 the lesion spectrum encompassing the presymptomatic phase of parkinson's disease: a
584 voltammetric study in the 6-ohda-lesioned rat. *Journal of neurochemistry* 87:1224–1236.

585 Berke JD (2018) What does dopamine mean? *Nature neuroscience* p. 1.

586 Borland LM, Shi G, Yang H, Michael AC (2005) Voltammetric study of extracellular dopamine
587 near microdialysis probes acutely implanted in the striatum of the anesthetized rat. *Journal*
588 *of neuroscience methods* 146:149–158.

589 Burt DR, Creese I, Snyder SH (1976) Properties of [3h] haloperidol and [3h] dopamine
590 binding associated with dopamine receptors in calf brain membranes. *Molecular pharma-*
591 *cology* 12:800–812.

592 Centonze D, Picconi B, Gubellini P, Bernardi G, Calabresi P (2001) Dopaminergic control of
593 synaptic plasticity in the dorsal striatum. *European journal of neuroscience* 13:1071–1077.

594 Cheer JF, Aragona BJ, Heien ML, Seipel AT, Carelli RM, Wightman RM (2007) Coordin-
595 ated accumbal dopamine release and neural activity drive goal-directed behavior. *Neu-*
596 *ron* 54:237–244.

597 Copeland RA (2004) *Enzymes: a practical introduction to structure, mechanism, and data*
598 analysis John Wiley & Sons.

599 Day JJ, Roitman MF, Wightman RM, Carelli RM (2007) Associative learning mediates dy-
600 namic shifts in dopamine signaling in the nucleus accumbens. *Nature neuroscience* 10:1020.

601 Day M, Wokosin D, Plotkin JL, Tian X, Surmeier DJ (2008) Differential excitability and mod-
602 ulation of striatal medium spiny neuron dendrites. *Journal of Neuroscience* 28:11603–11614.

603 DiResta G, Lee J, Lau N, Ali F, Galicich J, Arbit E (1990) Measurement of brain tissue density
604 using pycnometry In *Brain Edema VIII*, pp. 34–36. Springer.

605 Dreyer JK (2014) Three mechanisms by which striatal denervation causes breakdown of
606 dopamine signaling. *Journal of Neuroscience* 34:12444–12456.

607 Dreyer JK, Herrik KF, Berg RW, Hounsgaard JD (2010) Influence of phasic and tonic
608 dopamine release on receptor activation. *Journal of Neuroscience* 30:14273–14283.

609 Dreyer JK, Hounsgaard J (2013) Mathematical model of dopamine autoreceptors and uptake
610 inhibitors and their influence on tonic and phasic dopamine signaling. *Journal of neuro-
611 physiology* 109:171–182.

612 Everitt BJ, Robbins TW (2005) Neural systems of reinforcement for drug addiction: from
613 actions to habits to compulsion. *Nature neuroscience* 8:1481.

614 Flores-Barrera E, Vizcarra-Chacón BJ, Bargas J, Tapia D, Galarraga E (2011) Dopaminergic
615 modulation of corticostriatal responses in medium spiny projection neurons from direct and
616 indirect pathways. *Frontiers in systems neuroscience* 5:15.

617 Florescu SB, West AR, Ash B, Moore H, Grace AA (2003) Afferent modulation of dopamine
618 neuron firing differentially regulates tonic and phasic dopamine transmission. *Nature neu-
619 roscience* 6:968.

620 Frank MJ, O'Reilly RC (2006) A mechanistic account of striatal dopamine function in human
621 cognition: psychopharmacological studies with cabergoline and haloperidol. *Behavioral
622 neuroscience* 120:497.

623 Grace AA (1995) The tonic/phasic model of dopamine system regulation: its relevance
624 for understanding how stimulant abuse can alter basal ganglia function. *Drug & Alcohol*
625 *Dependence* 37:111–129.

626 Grace AA, Floresco SB, Goto Y, Lodge DJ (2007) Regulation of firing of dopaminergic
627 neurons and control of goal-directed behaviors. *Trends in neurosciences* 30:220–227.

628 Hamid AA, Pettibone JR, Mabrouk OS, Hetrick VL, Schmidt R, Vander Weele CM, Kennedy
629 RT, Aragona BJ, Berke JD (2016) Mesolimbic dopamine signals the value of work. *Nature*
630 *neuroscience* 19:117.

631 Howe MW, Tierney PL, Sandberg SG, Phillips PE, Graybiel AM (2013) Prolonged dopamine
632 signalling in striatum signals proximity and value of distant rewards. *Nature* 500:575–579.

633 Justice Jr J (1993) Quantitative microdialysis of neurotransmitters. *Journal of neuroscience*
634 *methods* 48:263–276.

635 Maeno H (1982) Dopamine receptors in canine caudate nucleus. *Molecular and cellular*
636 *biochemistry* 43:65–80.

637 Marcott PF, Mamaligas AA, Ford CP (2014) Phasic dopamine release drives rapid activation
638 of striatal d2-receptors. *Neuron* 84:164–176.

639 Mohebi A, Pettibone JR, Hamid AA, Wong J, Vinson LT, Patriarchi T, Tian L, Kennedy RT,
640 Berke JD (2019) Dissociable dopamine dynamics for learning and motivation. *Nature* .

641 Morris G, Arkadir D, Nevet A, Vaadia E, Bergman H (2004) Coincident but distinct messages
642 of midbrain dopamine and striatal tonically active neurons. *Neuron* 43:133–143.

643 Neve KA, Neve RL (1997) Molecular biology of dopamine receptors In *The dopamine recep-*
644 *tors*, pp. 27–76. Springer.

645 Nishikori K, Noshiro O, Sano K, Maeno H (1980) Characterization, solubilization, and sepa-
646 ration of two distinct dopamine receptors in canine caudate nucleus. *Journal of Biological*
647 *Chemistry* 255:10909–10915.

648 Niv Y, Daw ND, Joel D, Dayan P (2007) Tonic dopamine: opportunity costs and the control
649 of response vigor. *Psychopharmacology* 191:507–520.

650 Pan WX, Schmidt R, Wickens JR, Hyland BI (2005) Dopamine cells respond to predicted
651 events during classical conditioning: evidence for eligibility traces in the reward-learning
652 network. *Journal of Neuroscience* 25:6235–6242.

653 Pan WX, Schmidt R, Wickens JR, Hyland BI (2008) Tripartite mechanism of extinction
654 suggested by dopamine neuron activity and temporal difference model. *Journal of Neuro-
655 science* 28:9619–9631.

656 Patriarchi T, Cho JR, Merten K, Howe MW, Marley A, Xiong WH, Folk RW, Broussard GJ,
657 Liang R, Jang MJ et al. (2018) Ultrafast neuronal imaging of dopamine dynamics with
658 designed genetically encoded sensors. *Science* p. eaat4422.

659 Prou D, Gu WJ, Le Crom S, Vincent JD, Salamero J, Vernier P (2001) Intracellular retention of
660 the two isoforms of the d 2 dopamine receptor promotes endoplasmic reticulum disruption.
661 *Journal of Cell Science* 114:3517–3527.

662 Redgrave P, Rodriguez M, Smith Y, Rodriguez-Oroz MC, Lehericy S, Bergman H, Agid Y,
663 DeLong MR, Obeso JA (2010) Goal-directed and habitual control in the basal ganglia:
664 implications for parkinson's disease. *Nature Reviews Neuroscience* 11:760–772.

665 Reyes BA, Pendergast JS, Yamazaki S (2008) Mammalian peripheral circadian oscillators are
666 temperature compensated. *Journal of biological rhythms* 23:95–98.

667 Reynolds JN, Hyland BI, Wickens JR (2001) A cellular mechanism of reward-related learning.
668 *Nature* 413:67.

669 Richfield EK, Penney JB, Young AB (1989) Anatomical and affinity state comparisons between
670 dopamine d 1 and d 2 receptors in the rat central nervous system. *Neuroscience* 30:767–777.

671 Richfield EK, Young AB, Penney JB (1987) Comparative distribution of dopamine d-1 and
672 d-2 receptors in the basal ganglia of turtles, pigeons, rats, cats, and monkeys. *Journal of
673 Comparative Neurology* 262:446–463.

674 Robinson DL, Phillips PE, Budygin EA, Trafton BJ, Garris PA, Wightman RM (2001) Sub-
675 second changes in accumbal dopamine during sexual behavior in male rats. *Neurore-
676 port* 12:2549–2552.

677 Robinson SW, Jarvie KR, Caron MG (1994) High affinity agonist binding to the dopamine d3
678 receptor: chimeric receptors delineate a role for intracellular domains. *Molecular pharmacology* 46:352–356.

680 Roitman MF, Stuber GD, Phillips PE, Wightman RM, Carelli RM (2004) Dopamine operates
681 as a subsecond modulator of food seeking. *Journal of Neuroscience* 24:1265–1271.

682 Roitman MF, Wheeler RA, Wightman RM, Carelli RM (2008) Real-time chemical responses
683 in the nucleus accumbens differentiate rewarding and aversive stimuli. *Nature neuroscience* 11:1376.

685 Sano K, Noshiro O, Katsuda K, Nishikori K, Maeno H (1979) Dopamine receptors and
686 dopamine-sensitive adenylate cyclase in canine caudate nucleus: Characterization and sol-
687 ubilization. *Biochemical pharmacology* 28:3617–3627.

688 Schultz W (1998) Predictive reward signal of dopamine neurons. *Journal of neurophysiology*
689 80:1–27.

690 Schultz W (2007) Multiple dopamine functions at different time courses. *Annu. Rev. Neu-
691 rosci.* 30:259–288.

692 Schultz W (2016) Dopamine reward prediction-error signalling: a two-component response.
693 *Nature Reviews Neuroscience* 17:183.

694 Suaud-Chagny M, Chergui K, Chouvet G, Gonon F (1992) Relationship between dopamine
695 release in the rat nucleus accumbens and the discharge activity of dopaminergic neurons
696 during local in vivo application of amino acids in the ventral tegmental area. *Neuro-
697 science* 49:63–72.

698 Sun F, Zeng J, Jing M, Zhou J, Feng J, Owen SF, Luo Y, Li F, Wang H, Yamaguchi T et al.
699 (2018) A genetically encoded fluorescent sensor enables rapid and specific detection of
700 dopamine in flies, fish, and mice. *Cell* 174:481–496.

701 Surmeier DJ, Ding J, Day M, Wang Z, Shen W (2007) D1 and d2 dopamine-receptor mod-
702 ulation of striatal glutamatergic signaling in striatal medium spiny neurons. *Trends in
703 neurosciences* 30:228–235.

704 Syed EC, Grima LL, Magill PJ, Bogacz R, Brown P, Walton ME (2016) Action initiation
705 shapes mesolimbic dopamine encoding of future rewards. *Nature neuroscience* 19:34.

706 Syková E, Nicholson C (2008) Diffusion in brain extracellular space. *Physiological re-*
707 *views* 88:1277–1340.

708 Tobler PN, Fiorillo CD, Schultz W (2005) Adaptive coding of reward value by dopamine
709 neurons. *Science* 307:1642–1645.

710 Venton BJ, Zhang H, Garris PA, Phillips PE, Sulzer D, Wightman RM (2003) Real-time
711 decoding of dopamine concentration changes in the caudate–putamen during tonic and
712 phasic firing. *Journal of neurochemistry* 87:1284–1295.

713 Yapo C, Nair AG, Clement L, Castro LR, Hellgren Kotaleski J, Vincent P (2017) Detec-
714 tion of phasic dopamine by d1 and d2 striatal medium spiny neurons. *The Journal of*
715 *physiology* 595:7451–7475.

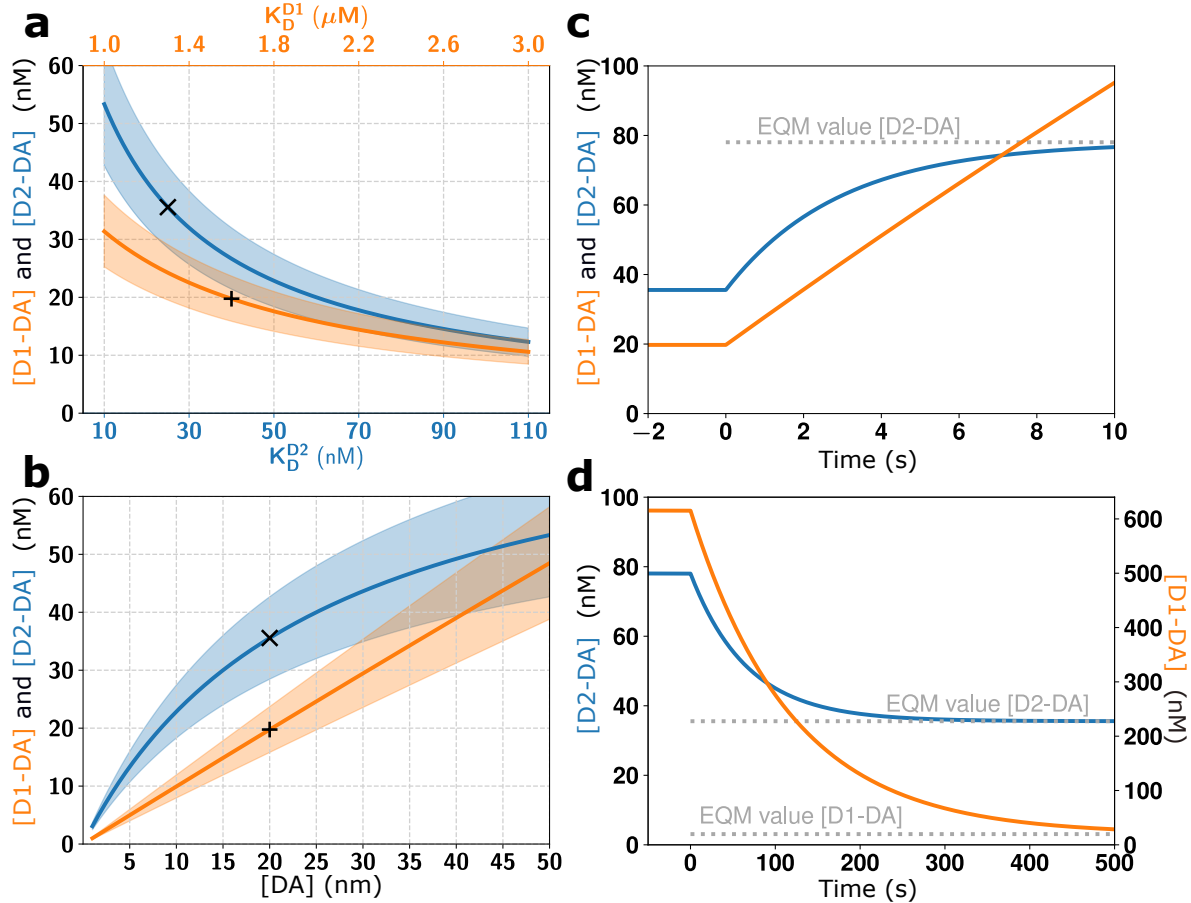


Figure 1: Baseline levels of D1 and D2 receptor occupation and impact of slow kinetics.

(a) Equilibrium values of absolute concentration of receptors bound to DA as a function of receptor affinities. Here, baseline $[DA]$ was fixed at 20 nM. **(b)** Equilibrium values of absolute concentration of receptors bound to DA as a function of baseline $[DA]$. Here $K_D^{D1} = 1.6 \mu M$ and $K_D^{D2} = 25 nM$. 'X' and '+' indicate the model default parameters. Coloured bands mark the range of values for up to ±20% different receptor abundances. **(c)** Temporal dynamics of D1 and D2 receptor occupancy for a large step up from $[DA] = 20 nM$ to $[DA] = 1 \mu M$. The gray dotted line shows that equilibrium value (EQM). **(d)** Same as in **c** but for a step down from $[DA] = 1 \mu M$ to $[DA] = 20 nM$.

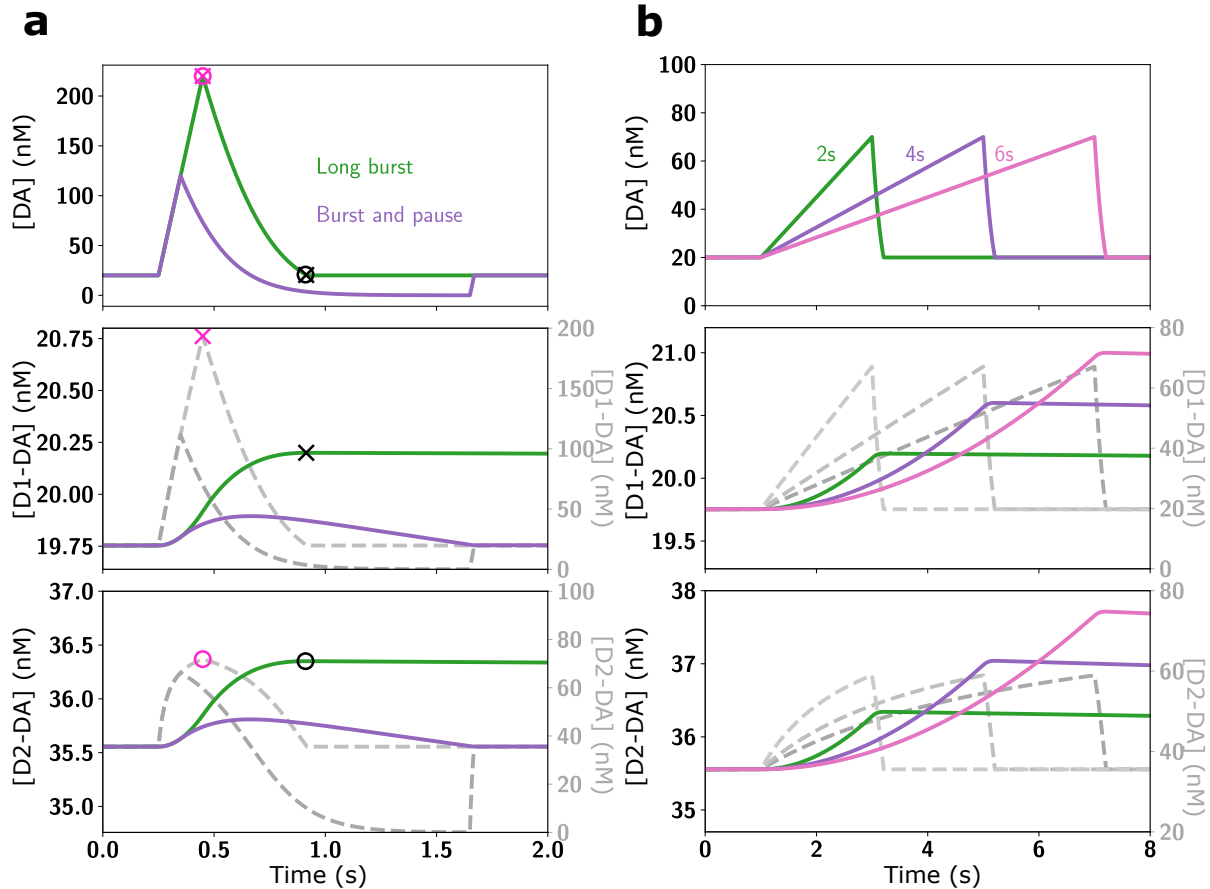


Figure 2: Impact of receptor kinetics on responses to different DA signals. **(a)** Two different DA signals, long burst and burst-pause, were simulated. The top panel shows the time course of the model [DA] input signal, with the resulting changes in D1 and D2 receptor occupancy in the middle and bottom panel, respectively. The colored traces in the middle and bottom panel show the resulting [DA-D1] and [DA-D2] for the realistic kinetics model (left scales), and the dashed gray traces show the corresponding values for the affinity-based model (right scales). The timing of the maximum receptor occupancy ('x' and 'o' for D1 and D2, respectively) coincides for instant kinetics (purple symbols) with the [DA] peak (combined x and o in top panel), while for slow kinetics (black symbols) it coincides with the offset of the [DA] signal instead (combined x and o in top panel). **(b)** Same as in (a) but for ramping DA signals.

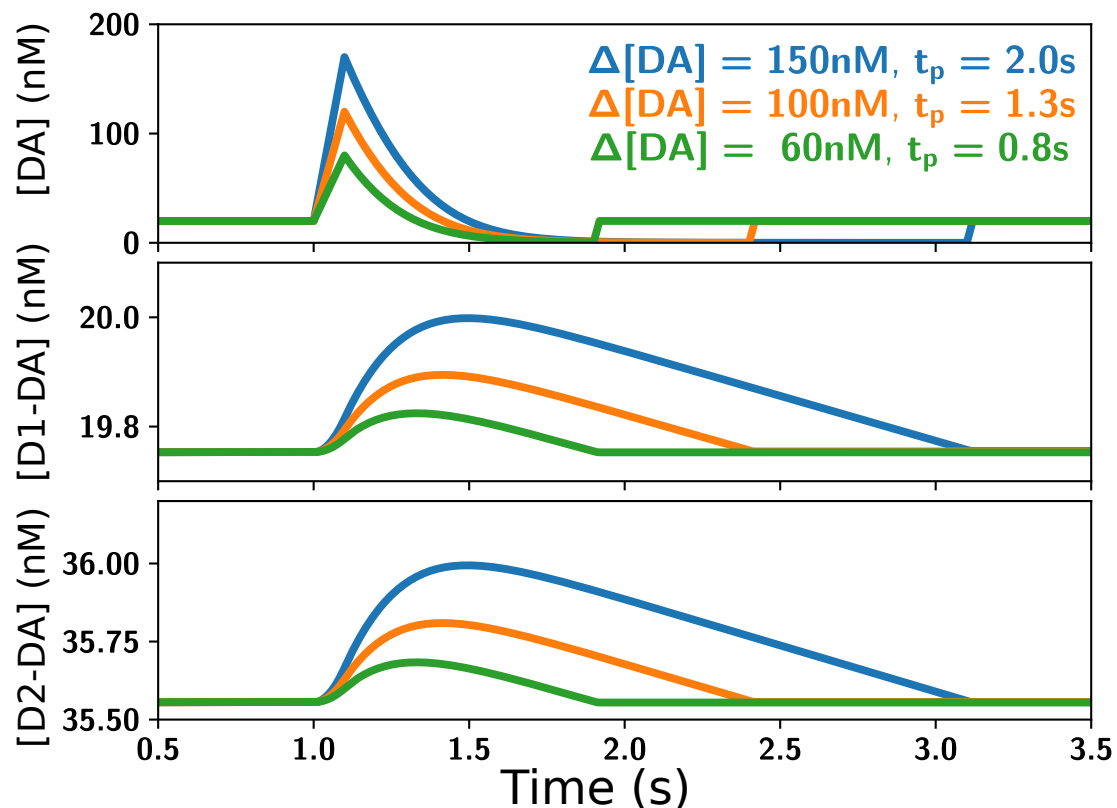


Figure 3: Burst-pause DA signals (top panel) did not lead to a prolonged D1 or D2 receptor occupation (middle and bottom panels, respectively). The initial increase in receptor occupation due to the burst component was quickly cancelled by the unbinding that occurred during the pause component. Higher burst amplitudes required a longer pause duration for the cancellation of the receptor occupation.

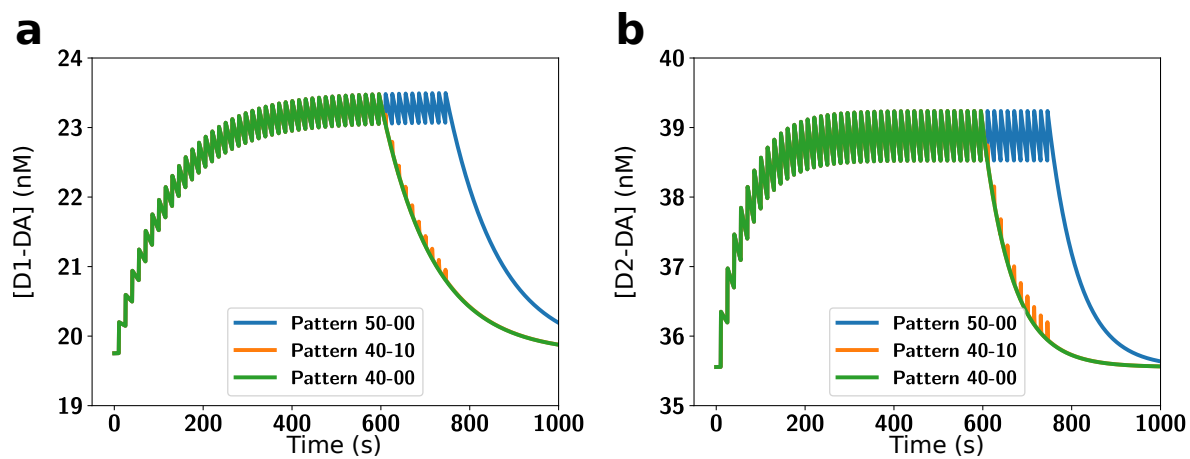


Figure 4: D1 and D2 receptor occupation integrates DA signals over a behavioural time scale.

(a) The absolute receptor occupancy for D1Rs for three different types of sequences consisting of 50 DA events each. The sequences consisted of 50 long burst events (blue), 40 long burst followed by 10 burst-pause events (orange) and 40 long burst events followed by 10 non-events (green, for comparison). **(b)** Same as in **a** but for D2Rs. Note that for the time course of the overall receptor occupation burst-pause signals are basically identical to non-events.

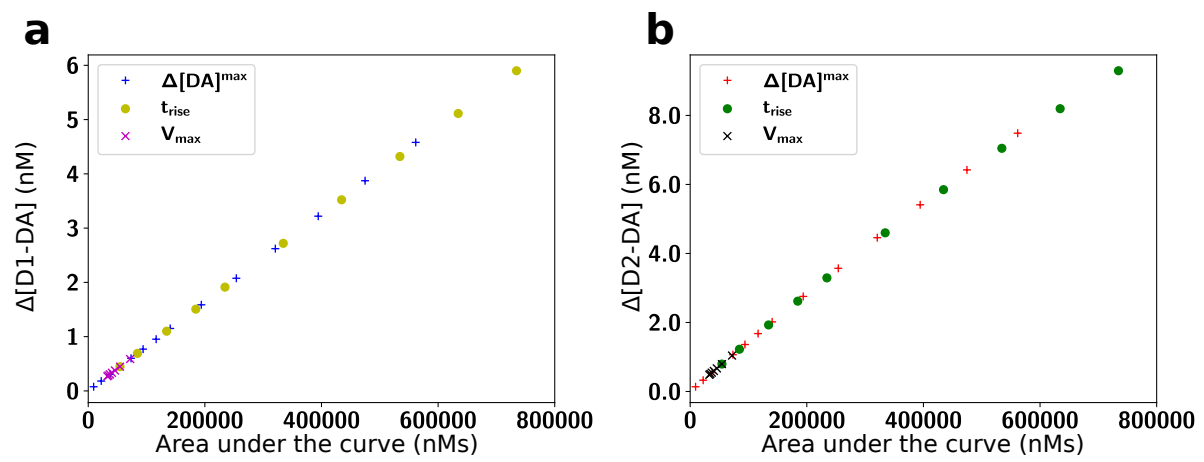


Figure 5: DA receptor occupation is proportional to the area under the curve of DA signals. The peak change in absolute receptor occupancy of D1Rs **(a)** and D2Rs **(b)** shown on the y-axis increased linearly with the area under the curve of the DA pulses. Each data point provides the result of a single simulation with a given parameter setting for the burst amplitude ($\Delta[DA]^{max}$), ramp rise time (t_{rise}), and DA re-uptake rate (V_{max}).

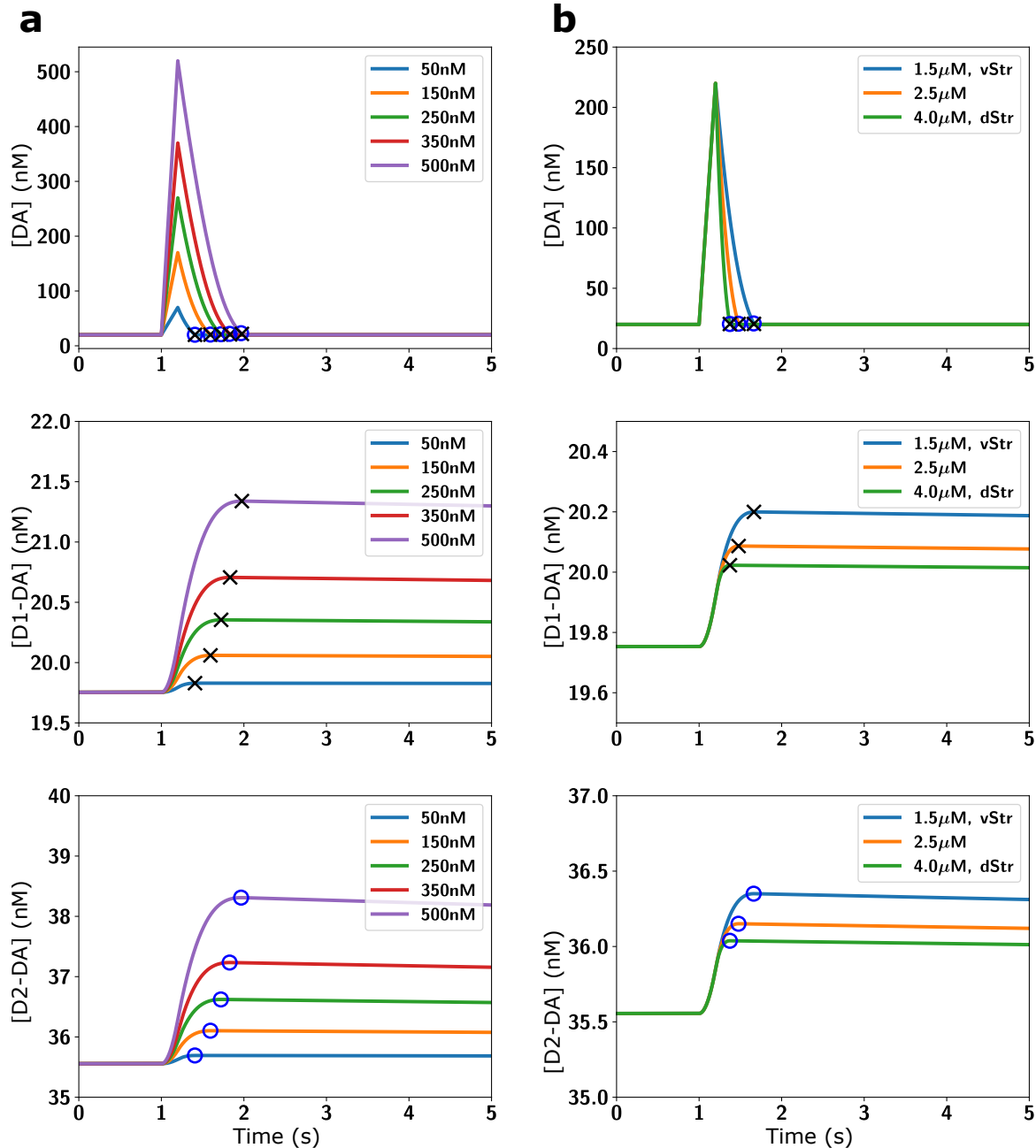


Figure 6: Parameter exploration for phasic DA bursts (top row) with the resulting changes in D1 (middle row) and D2 (bottom row) receptor occupancy. **(a)** Effect of variations in the amplitude $\Delta[DA]^{max}$ of the phasic DA burst (top row) on the D1 (middle row) and D2 (bottom row) receptor occupancy. **(b)** Effect of change in the re-uptake rate V_{max} rate (top row) on the D1 (middle row) and D2 (bottom row) receptor occupancy. V_{max} was changed to mimic conditions for the ventral and dorsal striatum. Blue circles and black crosses mark the time points of maximum receptor occupancy for D1 and D2, respectively. Note that for both D1R and D2R the time of maximum receptor occupancy was near the end of the DA signal and that D1Rs and D2Rs behaved similarly independent of the specific parameters of the DA pulse.

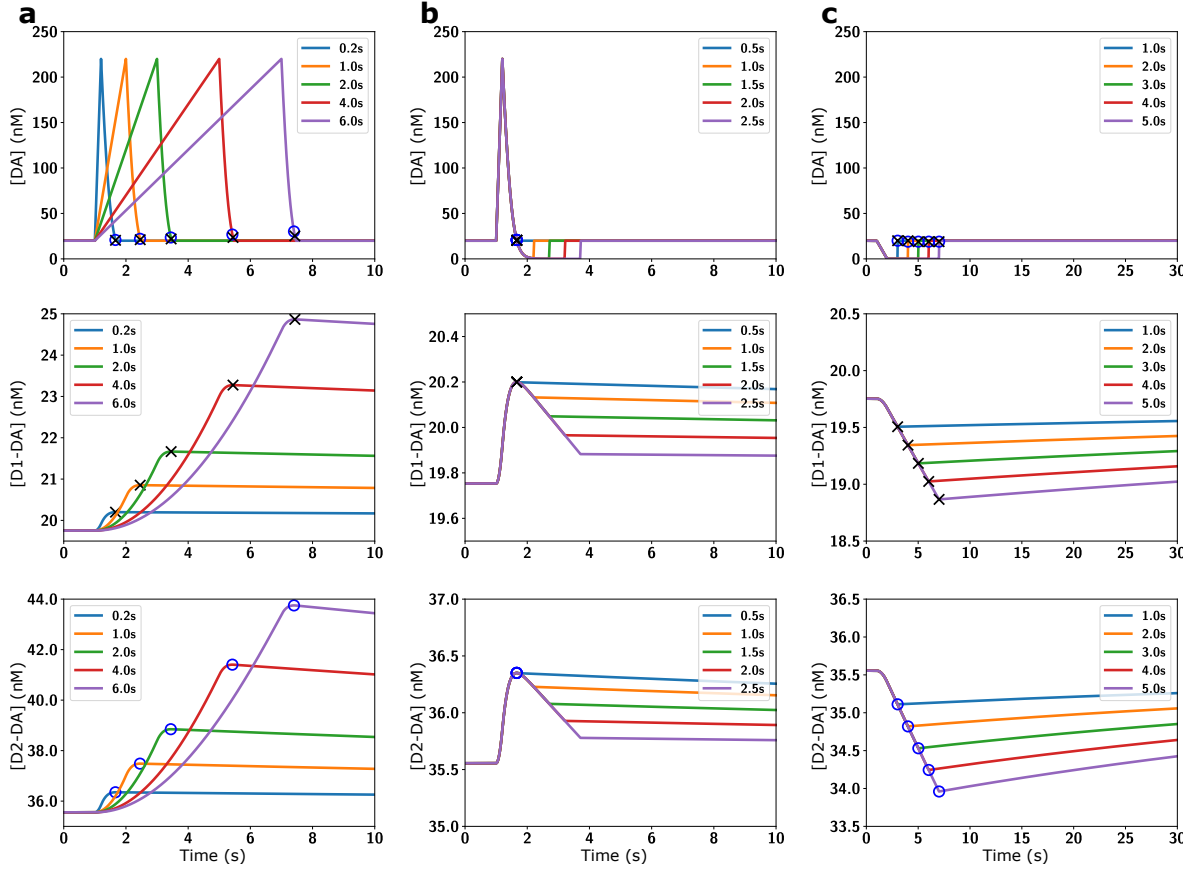


Figure 7: Parameter exploration for different DA signals (top row) with the resulting changes in D1 (middle row) and D2 (bottom row) receptor occupancy. **(a)** D1 (middle row) and D2 (bottom row) receptor occupancy for different rise time t_{rise} of the DA ramps (top row). The rise time controls the amount and duration of D1 (middle row) and D2 (bottom row) receptor occupancy. **(b)** D1 (middle row) and D2 (bottom row) receptor occupancy for different pause duration t_{pause} of the burst-pause type DA signals (top row). **(c)** D1 (middle row) and D2 (bottom row) receptor occupancy for different pause duration t_{pause} of DA pauses (without a preceding burst). Such a DA pause led to a fast reduction of receptor occupancy, which took 10s of seconds to return to baseline. The blue circles and black crosses mark the time points of maximum receptor occupancy for D1 and D2, respectively (a-b), or of minimal receptor activation (c). Note that for both D1R and D2R the time of maximum (or minimum for c) receptor occupancy was near the end of the DA signal and that D1Rs and D2Rs behaved similarly independent of the specific parameters of the DA pulse.

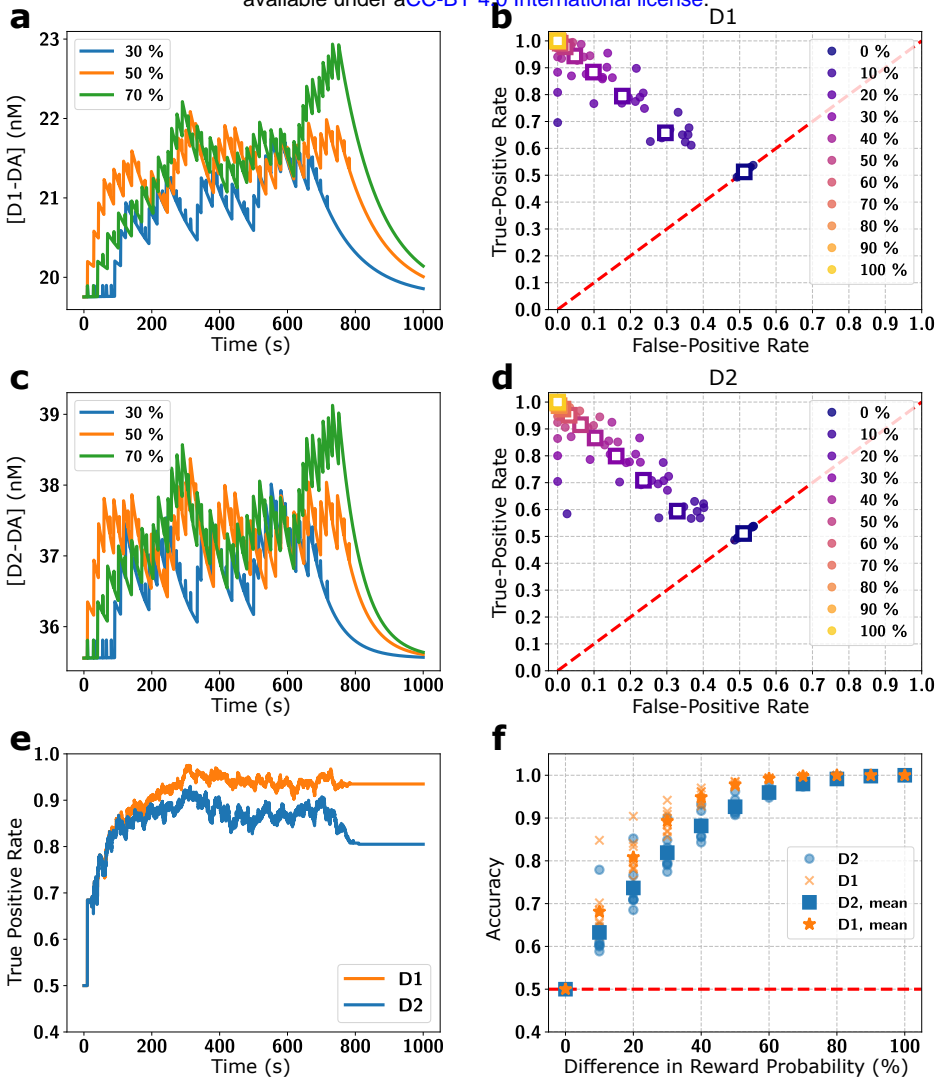


Figure 8: Encoding of reward rate by integration of DA signals over minutes in a simulation of a behavioural task. **(a)** Time course of D1 receptor occupancy for sequences of 50 trials with a reward probability, as indicated, in each trial. **(b)** True and false positive rates of the difference in reward probability based on the D1 and D2 receptor occupancy by a simple classifier. Each dot indicates the true and false positive rate from a simulation scenario with the difference in reward probability indicated by the colour. The colour indicates the difference in reward probability (e.g. a 10% difference in purple occurs for 80% vs. 90%, 70% vs. 80%, etc.), and the squares denote the corresponding averages. The red line indicates chance level performance, and a perfect classifier would be at 1.0 true and 0.0 false positive rate. **(c, d)** The same as in panels **a** and **b** but for D2 receptors. **(e)** True positive rates for the classification in a sample session (70% vs 30% reward probability) based on the receptor occupancy of D1 (orange) and D2 (blue) receptors. After a short “swing-in” the receptors distinguished between a 70% and a 30% reward rate. **(f)** Accuracy of the classifier for a range of reward probability differences for the D1 (orange) and D2 (blue) receptors for individual sessions and corresponding session averages.

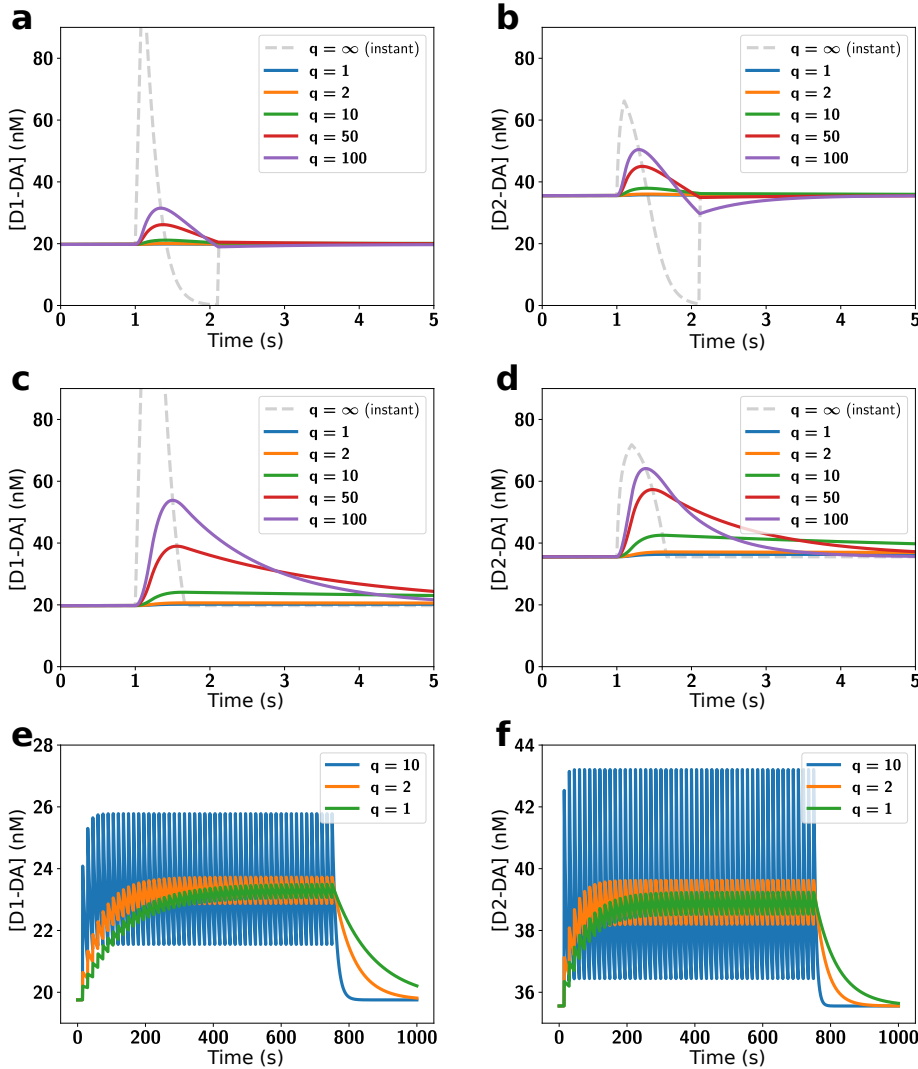


Figure 9: Similarities between D1 and D2 responses persist even if kinetics are much faster than our estimate. Absolute D1R occupancy ([D1-DA]; left column) and D2R occupancy ([D2-DA]; right column) were examined for burst-pause DA signals (**a, b**), burst-only DA signals (**c, d**), and the behavioural sequence (**e, f**) (i.e. same simulation scenarios as in Fig. 2a and the 50 bursts pattern from Fig. 4).

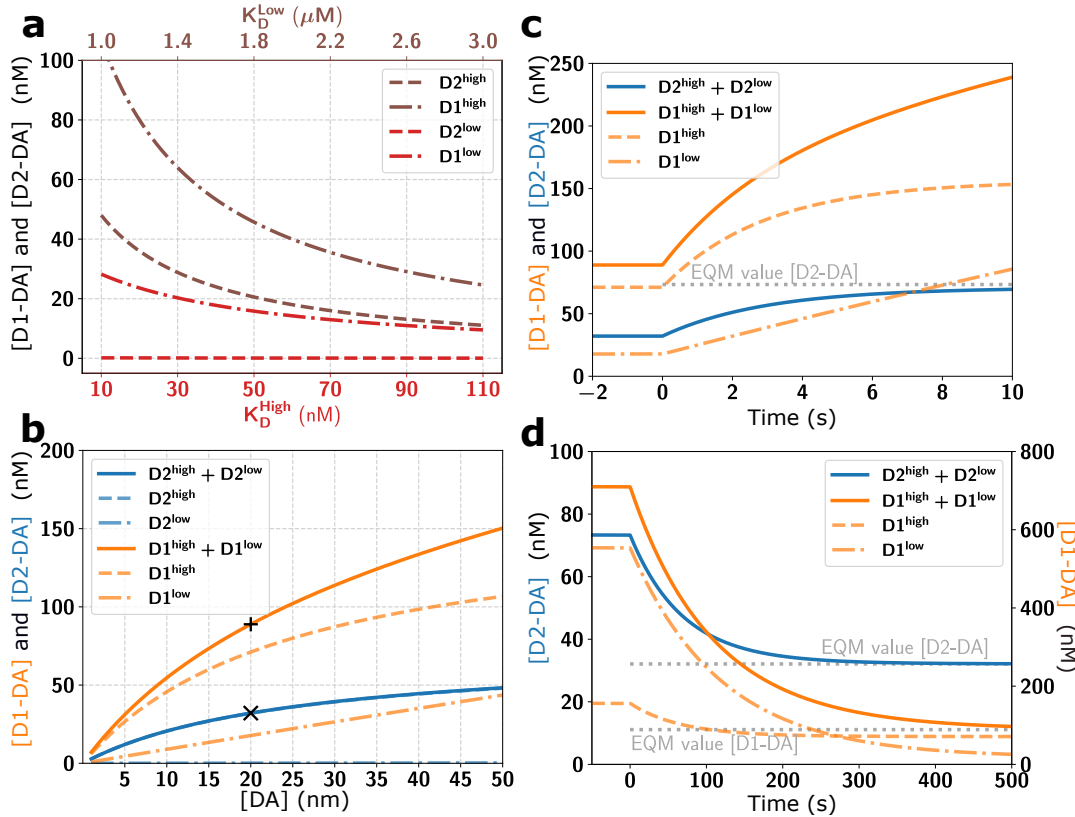


Figure 10: Baseline levels of D1 and D2 receptor occupation and impact of slow kinetics with different receptor affinity states. Here 10% of D1R are assumed to be in a high affinity state ($D1^{\text{high}}$) and 90% of D1R in a low affinity state ($D1^{\text{low}}$), while 10% of the D2R are in a low affinity state ($D2^{\text{low}}$) and 90% of D2R are in their high affinity state ($D2^{\text{high}}$). The overall receptor occupation for each receptor type is then the summed occupation of both states ($D1^{\text{high}} + D1^{\text{low}}$ and $D2^{\text{high}} + D2^{\text{low}}$). **(a)** The receptor occupancy at baseline $[DA] = 20\text{ nM}$ was dominated by the high affinity states for both receptors, even though only 10% of the D1R were in the high state. **(b)** The amount of bound D1R and D2R stayed within the same order of magnitude over a range of baseline $[DA]$. 'x' and '+' indicate the model default parameters. **(c)** As in the default model, for a large step up from $[DA] = 20\text{ nM}$ to $[DA] = 1\mu\text{M}$, and **(d)** a step down from $[DA] = 1\mu\text{M}$ to $[DA] = 20\text{ nM}$, D1 and D2 receptor occupancy approached their new equilibrium (EQM, grey dotted lines) only slowly (i.e. over seconds to minutes). As the $[D1\text{-DA}]$ changes were dominated by the $D1^{\text{high}}$ component, they were very similar to the D2R responses.

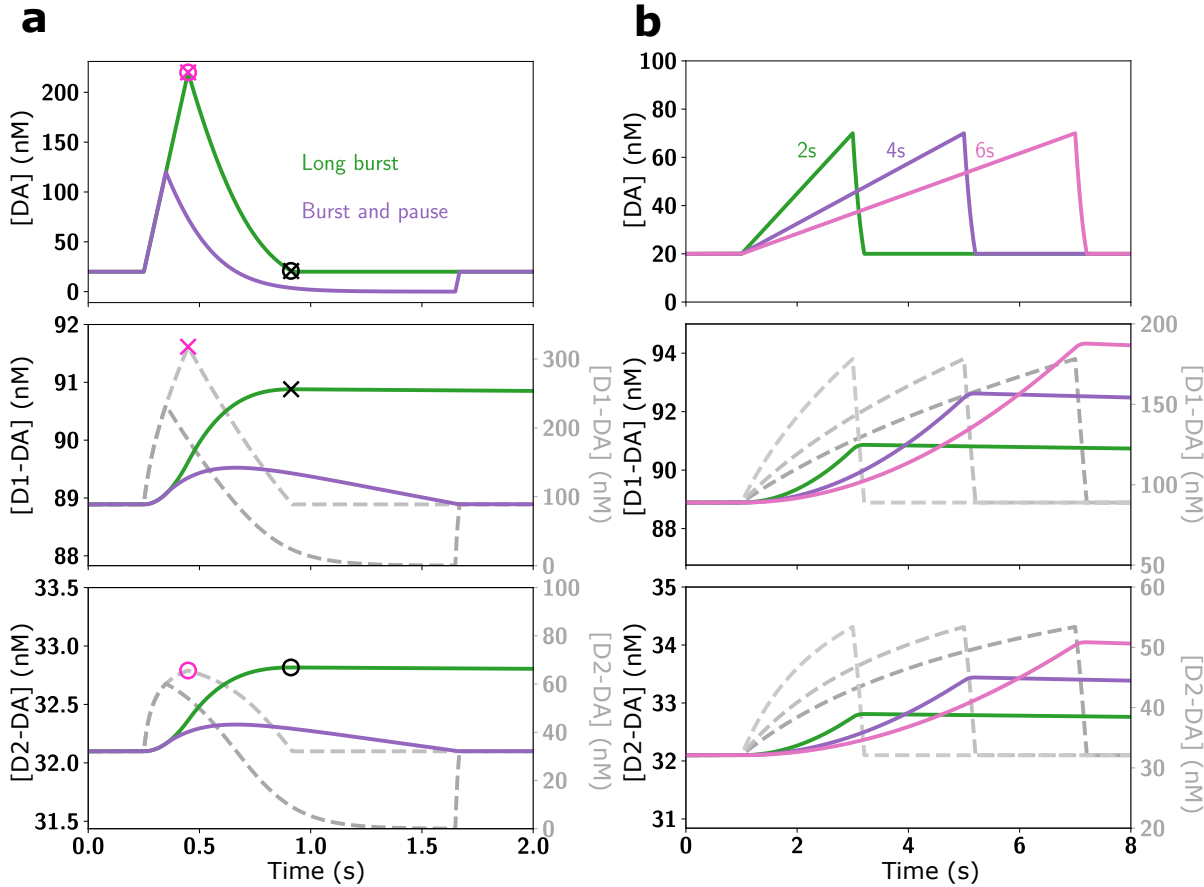


Figure 11: Impact of receptor kinetics on responses to different DA signals with 10% of D1R in a high affinity state ($D1^{high}$) and 10% of D2 receptors in a low affinity state ($D2^{low}$). **(a)** The effect of different phasic DA signals (top panels) on D1 (middle row) and D2 (bottom row) receptor occupancy in the slow kinetics model accounting for affinity states (coloured traces in middle and bottom panels; left scales) and to the affinity-based model (dashed grey traces, right scales). **(b)** Same as in the panel **a** but for DA ramps of different speed. As in the default model, the timing of the maximum receptor occupancy ('x' and 'o' for D1 and D2, respectively) coincides for instant kinetics (purple symbols) with the [DA] peak (combined x and o in top panel), while for slow kinetics (black symbols) it coincides with the offset of the [DA] signal instead (combined 'x' and 'o' in top row panel **a**). The main difference to the default model is the higher occupancy of the D1R, due to the $D1^{high}$ component. There is no two-component unbinding since the $D1^{high}$ and $D1^{low}$ have similar off-rates, but differing on-rates. Overall, also for receptors with two affinity states, DA ramps are very effective in occupying the receptors.

Measured values		
Parameter		Source
$[D1]^m$ in pmol/mg protein	2840	(Richfield et al., 1989)
$[D2]^m$ in pmol/mg protein	696	(Richfield et al., 1989)
ϵ	0.12	(Banay-Schwartz et al., 1992)
α	0.2	(Syková and Nicholson, 2008)
ρ_{brain} in g/ml	1.05	(DiResta et al., 1990)
$f_{D1}^{membrane}$	1.0	(Prou et al., 2001)
$f_{D2}^{membrane}$	0.2	(Prou et al., 2001)
$k_{on}^{D1,orig}$ in $nm^{-1}min^{-1}$	0.00025	(Sano et al., 1979)
$k_{off}^{D1,orig}$ in min^{-1}	0.64	(Sano et al., 1979)
k_{on}^{D2} in $nm^{-1}min^{-1}$	0.02	(Burt et al., 1976)
k_{off}^{D2} in min^{-1}	0.5	(Burt et al., 1976)

Derived Parameters		
Parameter		Source
$[D1]$ in nM	≈ 1600	Eq.(17)
$[D2]$ in nM	≈ 80	Eq.(17)
$k_{on}^{D1,used}$ in $nm^{-1}min^{-1}$	0.0003125	see Text
$k_{off}^{D1,used}$ in min^{-1}	0.5	see Text

Table 1: Receptor parameters